

Electronic Supplementary Information

Efficient energy transfer in heparin-based co-assemblies of donor-acceptor cyanostilbenes

Shubhra Kanti Bhaumik, Nitish Kumar and Supratim Banerjee*

Department of Chemical Sciences, Indian Institute of Science Education and Research Kolkata,
Mohanpur 741246, Nadia, India.

Email: supratim.banerjee@iiserkol.ac.in

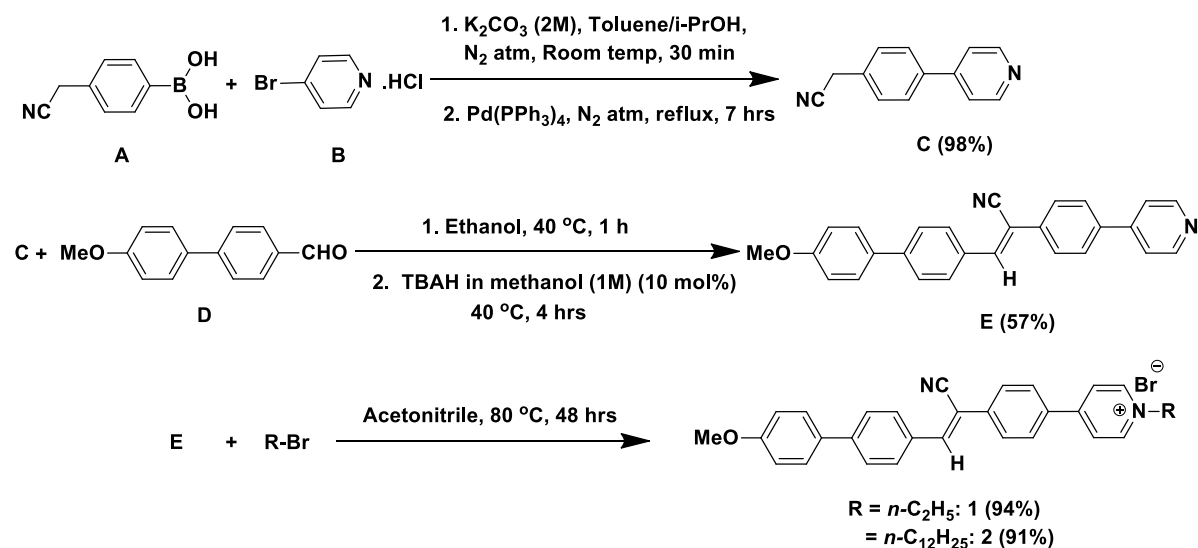
Table of Contents	Page No.
Experimental Procedure	S3
1. Materials and Method	S3
2. Synthetic Schemes and Characterization Data	S4
3. Preparation of Solutions	S5
4. Titration Procedures	S6
5. Quantum Yield Calculation Method	S7
6. Energy Transfer Efficiency Calculation	S7
7. Antenna Effect Calculation	S7
8. TEM Sample Preparation	S7
9. SEM Sample Preparation	S8
10. Limit of Detection (LOD) Calculation	S8
11. Gel Electrophoresis Measurement	S8
Results and Discussion	S8
1. Photo-physical Properties of 1 and 2	S8
2. Heparin Binding Studies of 1 and 2	S9
3. Energy Transfer Studies in Aqueous Buffer	S12
4. DLS Measurements	S22
5. Time-correlated Single Photon Counting (TCSPC) Measurements	S26
6. NMR Spectra	S27
Reference	S32

Experimental Procedures

1. Materials and Method:

All reagents were purchased from commercially available sources and used without further purification. 4'-methoxy-[1,1'-biphenyl]-4-carbaldehyde, (4-(cyanomethyl)phenyl)boronic acid and 4-bromopyridine hydrochloride were purchased from Combi-Blocks. Tetrakis(triphenylphosphine) palladium (0), tris(hydroxymethyl)aminomethane, chondroitin sulfate sodium salt from shark cartilage, hyaluronic acid sodium salt from *Streptococcus equi*, tetrabutylammonium hydroxide in methanol (1M), 1-bromododecane, tert-butanol, Nile Red and Nile Blue perchlorate were purchased from Sigma-Aldrich. Ethyl bromide was purchased from Spectrochem Pvt. Ltd. Heparin sodium salt from hog intestine was purchased from TCI chemicals. All other solvents used were from Merck. UV-Vis spectroscopic measurements were carried out in Agilent Technologies Cary 8454 spectrophotometer. Emission spectroscopic measurements were carried out in Horiba Fluoromax 4 spectrofluorometer. Absolute quantum yields were measured using integrating sphere fitted with a Edinburgh FLS1000 spectrofluorometer. Fluorescence images were taken under 365 nm UV lamp. DLS and zeta potential measurements were carried out using Malvern Zetasizer NanoZS. A Horiba Jobin Yvon Fluorocube instrument fitted with a 375 nm diode laser excitation source (with a temporal resolution of 0.2 ns) was used for the time-resolved fluorescence experiments applying the time-correlated single photon counting (TCSPC) method. ^1H and ^{13}C NMR were performed on Jeol 400 MHz and Bruker 500 MHz spectrometers. Mass spectra were recorded in a Bruker mass spectrometer. TEM images were recorded in a JEOL JEM2100 PLUS instrument. FESEM images were recorded in a ZEISS Sigma instrument. Gel electrophoresis was performed in a Select BioProducts Horizontal Electrophoresis System and images were recorded in a G:Box Chemi-XRQ Synoptics 4.0 MP transilluminator.

2. Synthetic Schemes and Characterization Data:



Scheme S1. Synthetic route for the preparation of **1** and **2**.

A. Synthesis of E: 2-(4-(pyridin-4-yl)phenyl)acetonitrile (**C**) was first synthesized from (4-(cyanomethyl)phenyl)boronic acid (**A**) and 4-bromopyridine hydrochloride (**B**) according to a literature procedure.¹ Then, (Z)-3-(4'-(4-(pyridin-4-yl)phenyl)-2-(4-(pyridin-4-yl)phenyl)acrylonitrile (**E**) was prepared by the following procedure. 2-(4-(pyridin-4-yl)phenyl)acetonitrile (**C**) (150 mg, 0.77 mmol) and 4'-methoxy-[1,1'-biphenyl]-4-carbaldehyde (**D**) (170 mg, 0.80 mmol) were taken in a 10 mL round bottom flask and 4 mL ethanol was added. The reaction mixture was stirred for 1 hour at 40 °C. Tetrabutylammonium hydroxide (TBAH) in methanol (0.08 mL, 1M) was first diluted by adding into 0.24 mL methanol and then the solution was added dropwise over a period of 15 min at 40 °C until the reaction mixture became faint maroon color. Stirring was continued for 4 more hours at 40 °C and then the reaction mixture was cooled to room temperature. The pale yellowish residue was obtained after drying the solvent. Finally, the product was purified by column chromatography (20% ethyl acetate in dichloromethane as eluent and silica gel as stationary phase). Weight of the product obtained- 171 mg, yield = 57%.

¹H NMR (500 MHz, DMSO-*D*₆): δ (ppm) = 8.68 (d, J = 9 Hz, 2H), 8.20 (s, 1H), 8.06 (d, J = 8 Hz, 2H), 7.99 (d, J = 8 Hz, 2H), 7.94 (d, J = 7.5 Hz, 2H), 7.85 (d, J = 8 Hz, 2H), 7.80 (d, J = 4.5 Hz, 2H), 7.75 (d, J = 8 Hz, 2H), 7.07 (d, J = 8 Hz, 2H), 3.82 (s, 3H).

¹³C NMR (125 MHz, DMSO-*D*₆): δ (ppm) = 159.55, 150.35, 145.82, 142.95, 141.94, 137.58, 134.70, 131.92, 131.15, 130.00, 127.99, 127.58, 126.47, 126.44, 121.11, 117.98, 114.54, 108.62, 55.24.

HRMS (ESI): m/z calculated for C₂₇H₂₁N₂O⁺ [(M-H)⁺]: 389.1648; found: 389.1653.

B. Synthesis of 1: E (50 mg, 0.13 mmol) and ethyl bromide (0.4 mL, 5.2 mmol) were taken in a 10 mL reaction tube and 1 mL acetonitrile was added to it. The reaction mixture was stirred at 80 °C under sealed conditions for 48 hours and then allowed to cool at room temperature. The solvent was removed and finally, the product (**1**) was purified by column chromatography (10-20% methanol in dichloromethane as eluent and silica gel as stationary phase). Weight of the product obtained- 61 mg, yield = 94%.

¹H NMR (400 MHz, DMSO-D₆): δ (ppm) = 9.16 (d, *J* = 5.6 Hz, 2H), 8.61 (d, *J* = 5.6 Hz, 2H), 8.31 (s, 1H), 8.27 (d, *J* = 7.2 Hz, 2H), 8.09 (d, *J* = 6.8 Hz, 2H), 8.05 (d, *J* = 7.2 Hz, 2H), 7.88 (d, *J* = 6.8 Hz, 2H), 7.76 (d, *J* = 7.2 Hz, 2H), 7.07 (d, *J* = 7.2 Hz, 2H), 4.64 (q, *J* = 6 Hz, 2H), 3.82 (s, 3H), 1.58 (t, *J* = 5.6 Hz, 3H).

¹³C NMR (125 MHz, DMSO-D₆): δ (ppm) = 159.61, 153.38, 144.64, 144.25, 142.26, 137.28, 133.73, 131.72, 131.04, 130.20, 128.93, 128.01, 126.73, 126.45, 124.46, 117.79, 114.55, 108.11, 55.55, 55.30, 16.33.

HRMS (ESI): m/z calculated for C₂₉H₂₅N₂O⁺: 417.1961; found: 417.1971.

C. Synthesis of 2: E (50 mg, 0.13 mmol) and n-dodecyl bromide (0.54 mL, 2.6 mmol) were taken in a 10 mL reaction tube and 1 mL acetonitrile was added to it. The reaction mixture was stirred at 80 °C under sealed condition for 48 hours and then allowed to cool at room temperature. The solvent was removed and finally the product (**2**) was purified by column chromatography (10-20% methanol in dichloromethane as eluent and silica gel as stationary phase). Weight of the product obtained- 72 mg, yield = 91%.

¹H NMR (400 MHz, DMSO-D₆): δ (ppm) = 9.14 (d, *J* = 6.8 Hz, 2H), 8.61 (d, *J* = 6.8 Hz, 2H), 8.31 (s, 1H), 8.27 (d, *J* = 8.8 Hz, 2H), 8.09 (d, *J* = 8.8 Hz, 2H), 8.05 (d, *J* = 8.8 Hz, 2H), 7.88 (d, *J* = 8.4 Hz, 2H), 7.77 (d, *J* = 8.8 Hz, 2H), 7.08 (d, *J* = 8.8 Hz, 2H), 4.59 (t, *J* = 7.2 Hz, 2H), 3.83 (s, 3H), 1.95 (quint, *J* = 4.4 Hz, 2H), 1.24-1.30 (br s, 18H), 0.85 (t, *J* = 7.2 Hz, 3H).

¹³C NMR (125 MHz, DMSO-D₆): δ (ppm) = 159.61, 153.40, 144.82, 144.25, 142.27, 137.30, 133.69, 131.66, 130.99, 130.20, 128.94, 128.01, 126.71, 126.46, 124.44, 117.83, 114.54, 108.06, 59.96, 55.24, 31.26, 30.63, 28.97, 28.88, 28.76, 28.67, 28.37, 25.41, 22.05, 13.91.

HRMS (ESI): m/z calculated for C₃₉H₄₅N₂O⁺: 557.3526; found: 557.3535.

3. Preparation of Solutions:

A. Preparation of Solutions of 1 and 2:

Initially, stock solutions of **1** and **2** were prepared by dissolving the solid powders in spectroscopic grade dimethyl sulfoxide (DMSO). These DMSO solutions were then diluted to

5 mM tris-HCl buffer made on Milli-Q water to get desired solutions having 1% DMSO as the final DMSO fraction. Solutions of **1** and **2** in aqueous buffer were then equilibrated for 30 min.

B. Preparation of Heparin Solution:

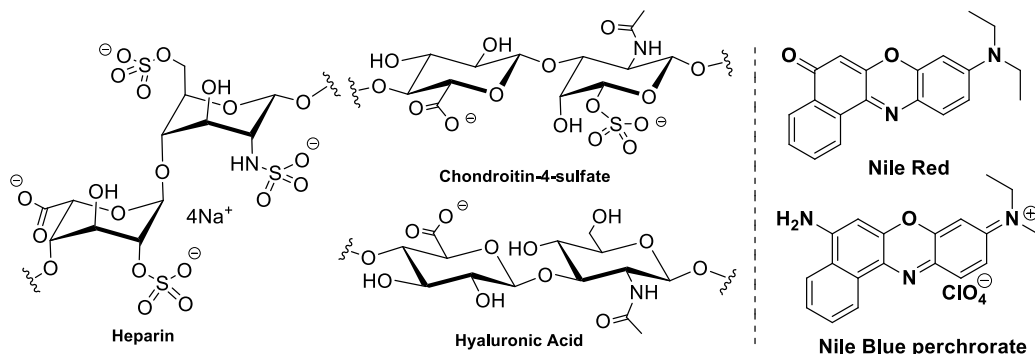


Fig. S1 Common repeat units of heparin, chondroitin-4-sulfate (**ChS**) and hyaluronic acid (**HA**). Chemical structures of Nile Red (**NR**) and Nile Blue perchlorate (**NB**).

The disaccharide unit shown in Fig. S1 is taken as the repeat unit of heparin for the molecular weight calculation. Though the supplied heparin contains only 30-40% materials with the active sequence of repeat units, the whole sample can still bind through the anionic polysaccharide unit irrespective of whether the repeat units are in active sequence or not. The molecular weight of the repeat unit is 665.40 g/mole. Heparin stock solutions were prepared in buffer and further diluted during titration.

C. Preparation of Solutions of Other Analytes:

Stock solutions of chondroitin-4-sulfate (**ChS**) and hyaluronic acid (**HA**) (structures are shown in Fig. S1) were prepared as 1.33 mg/mL in working buffer (2.7 mM for **ChS** and 3.3 mM for **HA**) and further diluted accordingly during titration.

D. Preparation of Nile Red and Nile Blue Solutions:

Stock solutions of Nile Red (**NR**) and Nile Blue (**NB**) (Fig. S1) were prepared in DMSO and further diluted accordingly during energy transfer studies.

4. Titration Procedures:

During the fluorometric titration, the addition of any of the analytes (heparin, chondroitin-4-sulfate or hyaluronic acid) was every time performed to a freshly equilibrated buffered solution of **1** or **2** to avoid any photoreaction of the cyanostilbene unit. After each addition of any analyte, 10 min equilibration time was given and then the spectrum was recorded. During energy transfer studies, solution of **NR** or **NB** was added to the pre-equilibrated solution of **1**, **2**, 1-heparin or 2-heparin in aqueous buffer.

5. Quantum Yield Calculation:

Absolute quantum yields of **1** (10 μM), **2** (10 μM) **1** (10 μM)-heparin (20 μM) and **2** (10 μM)-heparin (20 μM) in aqueous buffer were measured using an integrating sphere in a Edinburgh FLS1000 spectrometer.

6. Energy Transfer Efficiency Calculation:

Energy transfer (ET) efficiency is the percentage of the absorbed energy that is transferred to the acceptor and is expressed by the following equation

$$ET = (1 - I/I_0) \times 100\%$$

where, I and I_0 are the fluorescence intensities without and in presence of the acceptor in aqueous buffer.

7. Antenna Effect Calculation:

The antenna effect (AE) value under certain concentrations of donor and acceptor is the ratio of the emission intensities at the emission maximum of the acceptor in presence of the donor upon excitation of the donor and is expressed as follows-

$$AE = \frac{I_{D+A}(\lambda_{\text{ex}} = 365 \text{ nm}) - I_D(\lambda_{\text{ex}} = 365 \text{ nm})}{I_A(\lambda_{\text{ex}} = \text{abs maxima of A})}$$

where,

$I_{D+A}(\lambda_{\text{ex}} = 365 \text{ nm})$ = Emission intensity of acceptor in the presence of donor upon the excitation of donor

$I_D(\lambda_{\text{ex}} = 365 \text{ nm})$ = Emission intensity of donor in the absence of acceptor upon the excitation of donor

$I_A(\lambda_{\text{ex}} = \text{abs maxima of A})$ = Emission intensity of acceptor in the presence of donor upon the excitation of acceptor

8. TEM Sample Preparation:

3 μL of freshly prepared and equilibrated samples of **1**, **2**, **1-Hep**, and **2-Hep** in aqueous buffer were placed on the TEM grids (Ted Pella, Copper, Support films, Carbon type B, 300 mesh). The samples were placed for about 1 min and then the excess solvent was carefully wiped away from the corners of the grids by using soft paper tissues. Finally, the grids were kept under high vacuum for about 48 hours in order to dry them properly. Subsequently, the TEM images were recorded in a JEOL JEM2100 PLUS instrument.

9. SEM Sample Preparation:

5 μL of the freshly prepared and equilibrated solution of **2** in aqueous buffer was dropped on a small silicon wafer (Ted Pella) and kept for about 1 min. Then, the excess solvent was carefully wiped away from the wafer by soft tissue. Finally, the wafer was kept under a vacuum for 48 hours for drying them. The wafer was again dried for about 2 hours before recording in a Zeiss Sigma microscope.

10. Limit of Detection (LOD) Calculation:

Limit of detection was calculated using the equation 1.

$$\text{Limit of detection (LOD)} = 3\sigma/m \quad \dots \text{(equation 1)}^2$$

where, σ is the standard deviation of the intensity of free **1** or **2** (at their emission maxima in buffer) (determined based on five measurements), and m is the slope of the intensity (at their emission maxima in buffer) vs the concentration of heparin plot.

11. Gel Electrophoresis Measurement:

Agarose gel (0.6%) in TAE (tris-acetate-EDTA) buffer (1X, pH 8.6) was prepared with a previously reported fluorescent dye **CS6** (5 μM) as a staining dye. 10 μL of the samples (**Hep**, **1-Hep**, and **2-Hep**) were layered with a micropipette. The run was carried out in TAE buffer (1X, pH 8.6) by applying a voltage of 58 V for 45 mins using a Select BioProducts Horizontal Electrophoresis System. After migration, the plate was dried and the images were taken in a G:Box Chemi-XRQ Synoptics 4.0 MP transilluminator.

Results and Discussion

1. Photo-physical Properties of **1** and **2**:

Table S1. Lifetime data of **1** and **2** in DMSO and in aqueous buffer ($\lambda_{\text{ex}} = 375 \text{ nm}$).

System	λ_{em}	Lifetime (τ) parameters	Average lifetime (τ_{avg})	χ^2
1 (10 μM) in DMSO	585 nm	<0.2 ns (100%)	<0.2 ns	1.07
2 (10 μM) in DMSO	585 nm	0.21 ns (100%)	0.21 ns	1.09
1 (10 μM) in aqueous buffer	570 nm	$\tau_1 = 0.86 \text{ ns}$ (52%) $\tau_2 = 6.02 \text{ ns}$ (48%)	3.34 ns	1.10
2 (10 μM) in aqueous buffer	590 nm	$\tau_1 = 0.92 \text{ ns}$ (38%) $\tau_2 = 3.53 \text{ ns}$ (62%)	2.54 ns	1.13

Table S2. Size and kilo count per second (KCPS) of **1** and **2** in aqueous buffer

Compound	Size (nm)	KCPS
1 (4 μM)	130	154
2 (0.5 μM)	162	193

2. Heparin Binding Studies of 1 and 2:

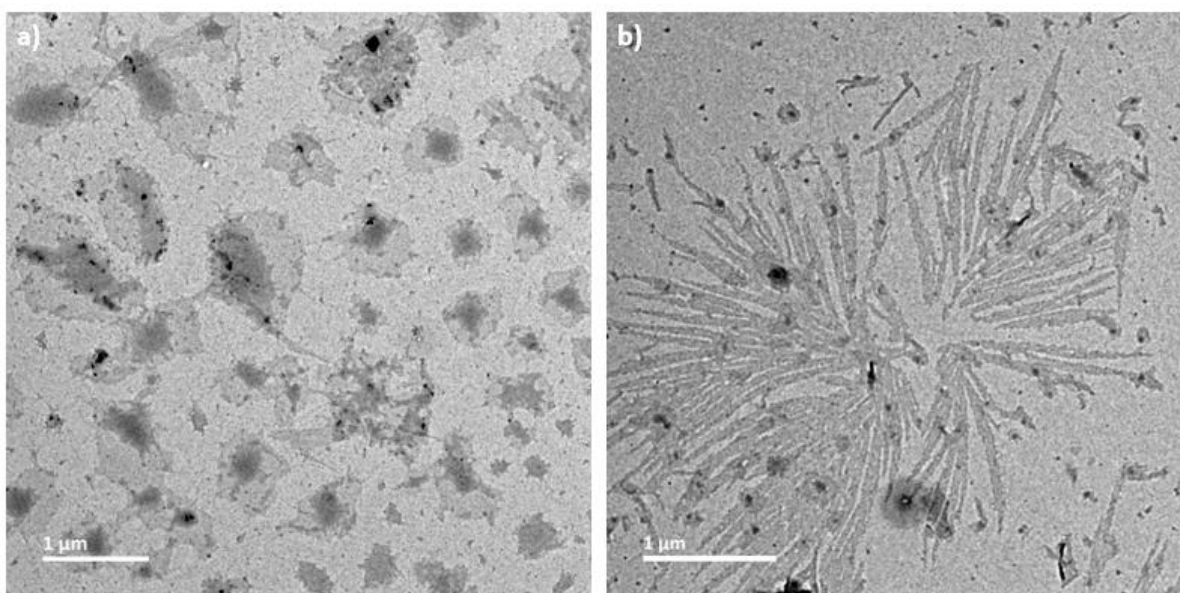


Fig. S2. Transmission electron microscopic (TEM) images of (a) **1-Hep** co-assembly and (b) **2-Hep** co-assembly obtained after drying from their aqueous solution (0.1% uranyl acetate as staining agent).

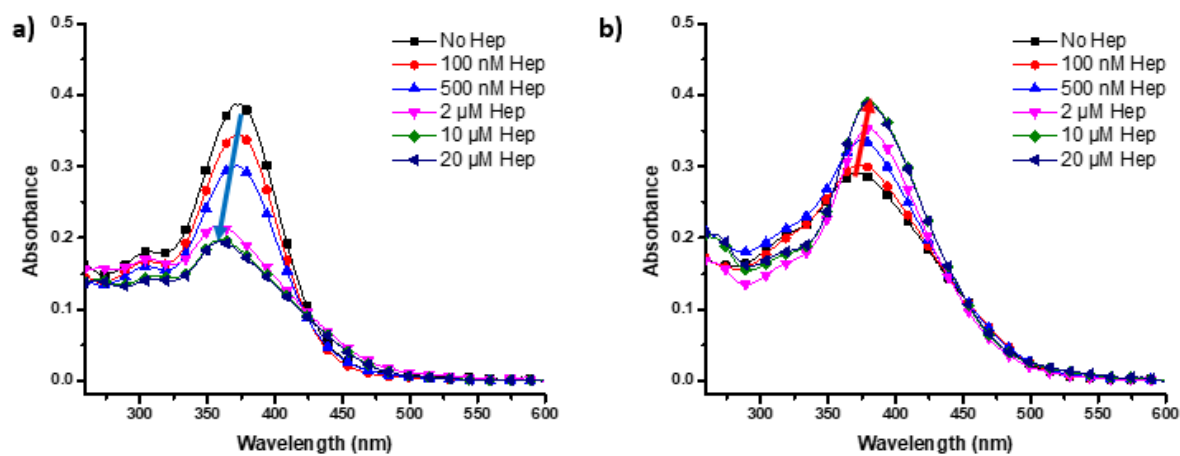


Fig. S3. Absorption spectral changes of (a) **1** (10 μM) and (b) **2** (10 μM) without and with different concentration of heparin (**Hep**) in aqueous buffer.

Table S3. Lifetime data of **1** and **2** in presence of heparin (**Hep**) in aqueous buffer ($\lambda_{\text{ex}} = 375$ nm).

System	λ_{em}	Lifetime (τ) parameters	Average lifetime (τ_{avg})	χ^2
1 (10 μM)- Hep (20 μM)	585 nm	$\tau_1 = 1.79$ ns (26%) $\tau_2 = 8.24$ ns (74%)	6.55 ns	1.23
2 (10 μM)- Hep (20 μM)	572 nm	$\tau_1 = 2.40$ ns (20%) $\tau_2 = 8.31$ ns (80%)	7.13 ns	1.05

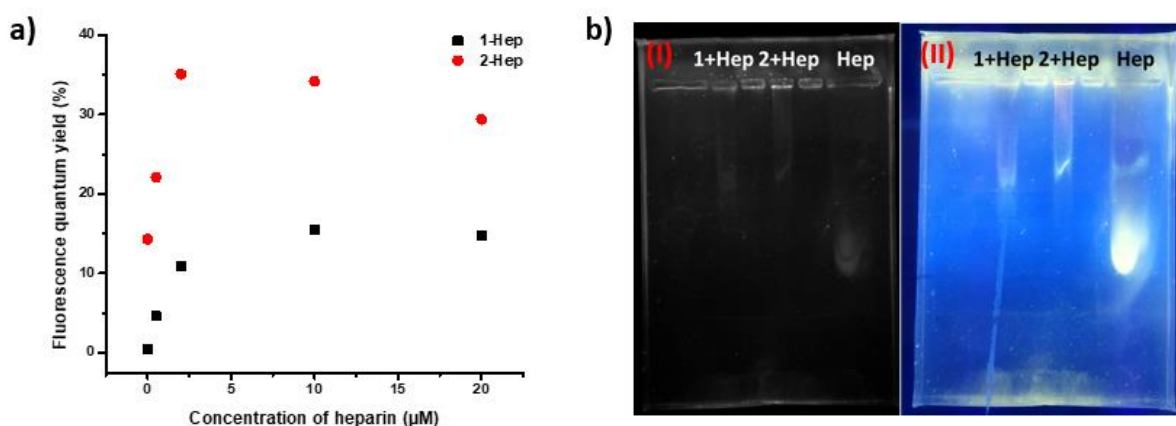


Fig. S4. (a) Fluorescence quantum yields of **1** (10 µM) and **2** (10 µM) in the presence of different amounts of heparin. (b) (I) Agarose-gel electrophoresis traces of **Hep**, **1-Hep** and **2-Hep**. [(II) Images of the traces taken under 365 nm UV].

Limit of detection (LOD) calculation:

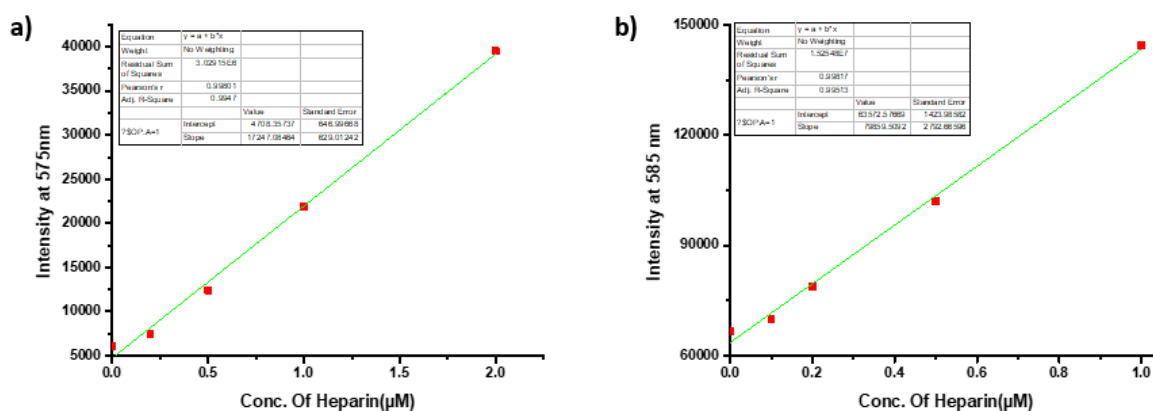


Fig. S5. Linear fit of fluorescence intensity vs heparin concentration for (a) **1** (10 µM) and (b) **2** (10 µM) in aqueous buffer.

LOD using 1: Standard deviation (σ) at 575 nm without heparin = 91.33

Slope of the linear fit (m) = 17247.08

Limit of Detection (LOD) = $3\sigma/m = 16$ nM (10.3 ng/mL)

LOD using 2: Standard deviation (σ) at 585 nm without heparin = 1049.56

Slope of the linear fit (m) = 79859.51

Limit of Detection (LOD) = $3\sigma/m = 39$ nM (25.1 ng/mL)

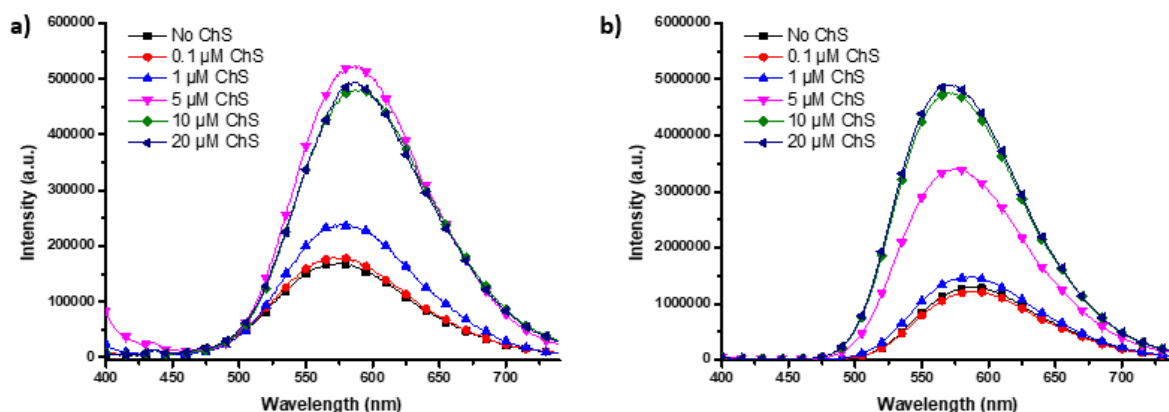


Fig. S6. Emission spectral changes of (a) **1** (10 μM) and (b) **2** (10 μM) without and with different concentration of chondroitin-4-sulfate (**ChS**) in aqueous buffer.

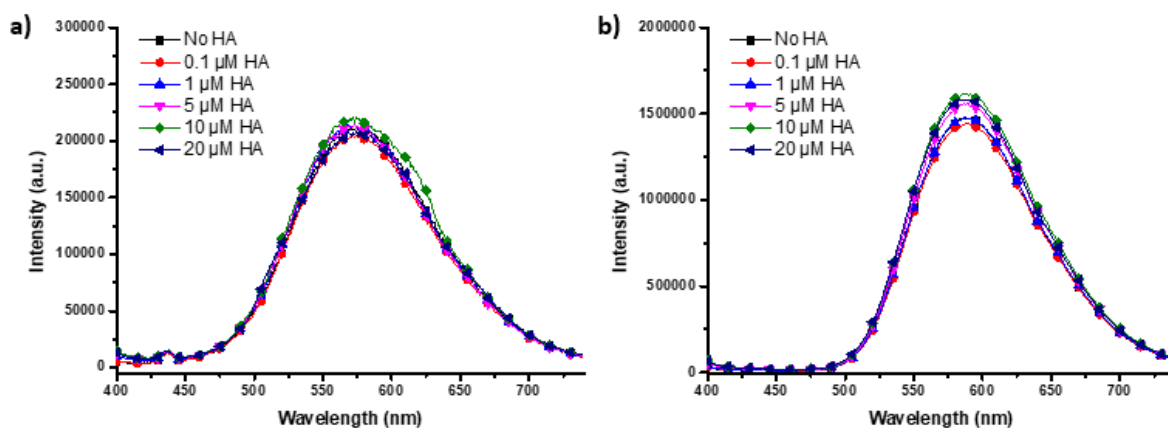


Fig. S7. Emission spectral changes of (a) **1** (10 μM) and (b) **2** (10 μM) without and with different concentration of hyaluronic acid (**HA**) in aqueous buffer.

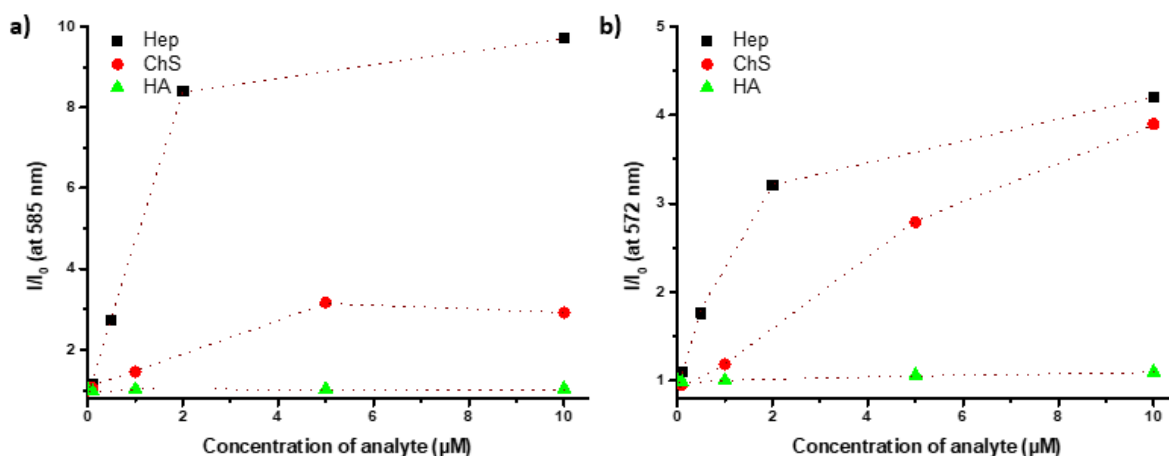


Fig. S8. Comparison of I/I_0 for (a) **1** (10 μM , at 585 nm) and (b) **2** (10 μM , at 572 nm) with different concentration of heparin (**Hep**), chondroitin-4-sulfate (**ChS**) and hyaluronic acid (**HA**) in aqueous buffer.

3. Energy Transfer Studies in Aqueous Buffer:

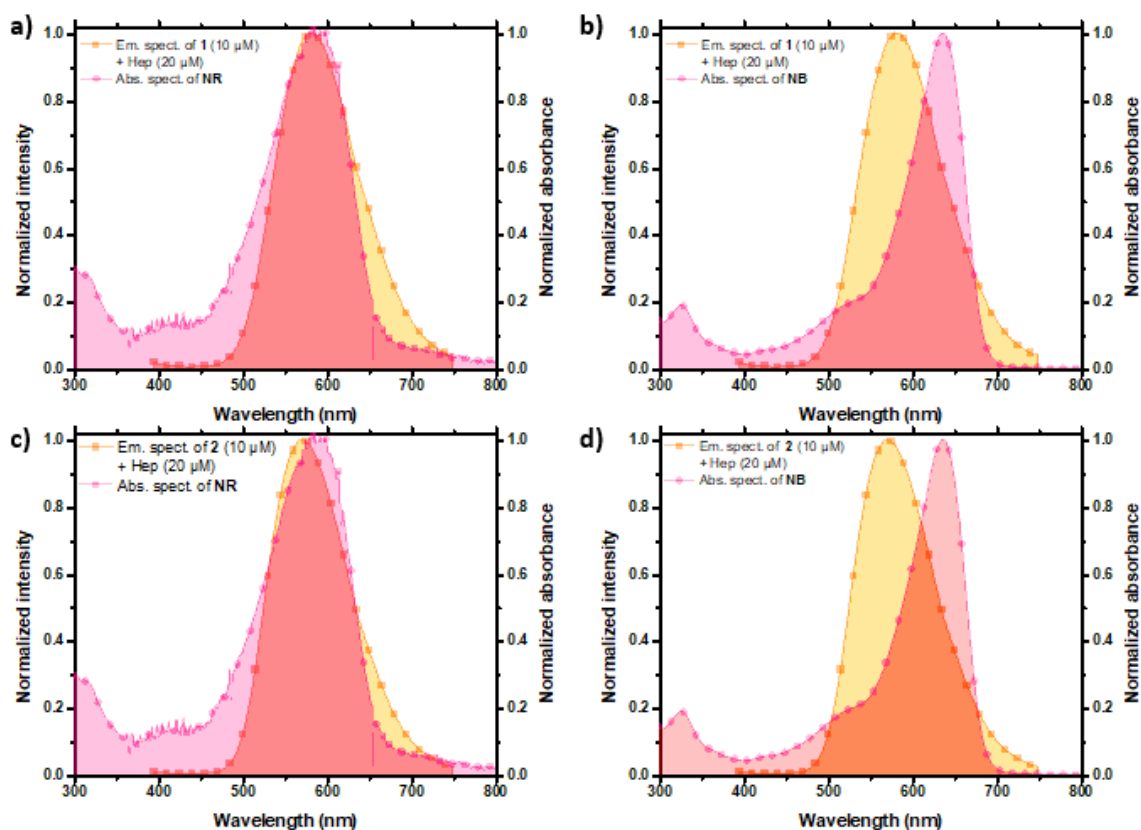


Fig. S9. Spectral overlap of emission of **1** (10 μM)-**Hep** (20 μM) and absorption of (a) Nile Red (**NR**) and (b) Nile Blue (**NB**) in aqueous buffer. Spectral overlap of emission of **2** (10 μM)-**Hep** (20 μM) and absorption of (c) Nile Red (**NR**) and (d) Nile Blue (**NB**) in aqueous buffer.

Spectral overlap between the co-assemblies and the acceptor dyes:

The overlap integral $[J(\varepsilon)]$ values of the emission spectra of the co-assemblies and the absorption spectra of the acceptor dyes were calculated by FluorTools software.

Table S4. Overlap integral $[J(\varepsilon)]$ of the emission spectrum of **1** (10 μM)-**Hep** (20 μM) and **2** (10 μM)-**Hep** (20 μM) and the absorption spectra of the acceptor dyes

Co-assembly	Nile Red (NR)	Nile Blue (NB)
1 (10 μM)- Hep (20 μM)	$9.84 \times 10^{-14} \text{ M}^{-1}\text{cm}^3$	$7.28 \times 10^{-13} \text{ M}^{-1}\text{cm}^3$
2 (10 μM)- Hep (20 μM)	$9.90 \times 10^{-14} \text{ M}^{-1}\text{cm}^3$	$6.73 \times 10^{-13} \text{ M}^{-1}\text{cm}^3$

Calculation of the radiative rate constant (k_r) for **1** (10 μM)-Hep (20 μM):

The radiative rate constant (k_r) of the donor [**1** (10 μM)-Hep (20 μM)] is calculated using the following equation: $k_r = Q_D/\tau$

where, Q_D = Quantum efficiency of the donor [**1** (10 μM)-Hep (20 μM)] = 0.1476

τ = Average lifetime of the donor [**1** (10 μM)-Hep (20 μM)] = 6.55 ns

The radiative rate constant (k_r) of [**1** (10 μM)-Hep (20 μM)] is determined to be $2.26 \times 10^7 \text{ s}^{-1}$.

Förster radius (R_0) calculation for **1** (10 μM)-Hep (20 μM) and NR/NB:

For any FRET system, Förster Radius (R_0) is calculated by using the following equation-

$$R_0 = 9.78 \times 10^3 \times [k^2 \times n^{-4} \times Q_D \times J(\epsilon)]^{1/6} \text{ in } \text{Å}$$

where,

k^2 = Relative orientation in space of the transition dipoles of donor and acceptors which is usually assumed to be 2/3.

n = refractive index of the medium = 1.33 for aqueous buffer

Q_D = Quantum efficiency of donor [**1** (10 μM)-Hep (20 μM)] = 0.1476

$J(\epsilon)_{NR}$ = Overlap integral of emission spectra of donor [**1** (10 μM)-Hep (20 μM)] and absorption spectra of acceptor [Nile Red (**NR**)] = $9.84 \times 10^{-14} \text{ M}^{-1}\text{cm}^3$

$J(\epsilon)_{NB}$ = Overlap integral of emission spectra of donor [**1** (10 μM)-Hep (20 μM)] and absorption spectra of acceptor [Nile Blue (**NB**)] = $7.28 \times 10^{-13} \text{ M}^{-1}\text{cm}^3$

R_0 for **1** (10 μM)-Hep (20 μM)-**NR** was calculated to be 37.18 Å (~3.72 nm).

R_0 for **1** (10 μM)-Hep (20 μM)-**NB** was calculated to be 51.90 Å (~5.19 nm).

Calculation of the radiative rate constant (k_r) for **2** (10 μM)-Hep (20 μM):

The radiative rate constant (k_r) of the donor [**2** (10 μM)-Hep (20 μM)] is calculated using the following equation: $k_r = Q_D/\tau$

where, Q_D = Quantum efficiency of the donor [**2** (10 μM)-Hep (20 μM)] = 0.2944

τ = Average lifetime of the donor [**2** (10 μM)-Hep (20 μM)] = 7.13 ns

The radiative rate constant (k_r) of [**2** (10 μM)-Hep (20 μM)] is determined to be $4.13 \times 10^7 \text{ s}^{-1}$.

Förster radius (R_0) calculation for **2** (10 μM)-Hep (20 μM) and NR/NB:

For any FRET system, Förster Radius (R_0) is calculated by using the following equation-

$$R_0 = 9.78 \times 10^3 \times [k^2 \times n^{-4} \times Q_D \times J(\epsilon)]^{1/6} \text{ in } \text{Å}$$

where,

k^2 = Relative orientation in space of the transition dipoles of donor and acceptors which is usually assumed to be $2/3$.

n = refractive index of the medium = 1.33 for aqueous buffer

Q_D = Quantum efficiency of donor [**2** (10 μM)-**Hep** (20 μM)] = 0.2944

$J(\epsilon)_{NR}$ = Overlap integral of emission spectra of donor [**2** (10 μM)-**Hep** (20 μM)] and absorption spectra of acceptor [Nile Red (**NR**)] = $9.90 \times 10^{-14} \text{ M}^{-1}\text{cm}^3$

$J(\epsilon)_{NB}$ = Overlap integral of emission spectra of donor [**2** (10 μM)-**Hep** (20 μM)] and absorption spectra of acceptor [Nile Blue (**NB**)] = $6.73 \times 10^{-13} \text{ M}^{-1}\text{cm}^3$

R_0 for **2** (10 μM)-heparin (20 μM)-**NR** was calculated to be 41.93 \AA ($\sim 4.19 \text{ nm}$).

R_0 for **2** (10 μM)-heparin (20 μM)-**NB** was calculated to be 57.76 \AA ($\sim 5.78 \text{ nm}$).

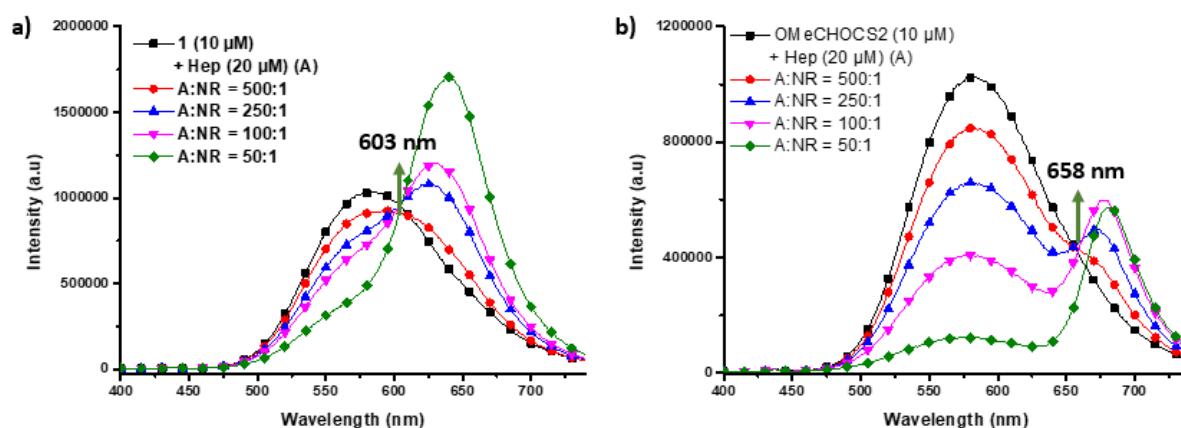


Fig. S10. Emission spectral changes of **1** (10 μM)-**Hep** (20 μM) in presence of (a) **NR** and (b) **NB** at different D/A ratio in aqueous buffer.

Table S5. ET efficiency (%) and Antenna effect (AE) values in **1** (10 μM)-**Hep** (20 μM)-**NR** system at different donor/acceptor ratios.

Donor/acceptor ratio	ET efficiency	AE
500:1	12%	24
250:1	20%	42
100:1	26%	37
50:1	48%	32

Table S6. ET efficiency (%) and Antenna effect (AE) values in **2** (10 μ M)-**Hep** (20 μ M)-**NR** system at different donor/acceptor ratios.

Donor/acceptor ratio	ET efficiency	AE
500:1	12%	23
250:1	23%	38
100:1	53%	51
50:1	78%	38

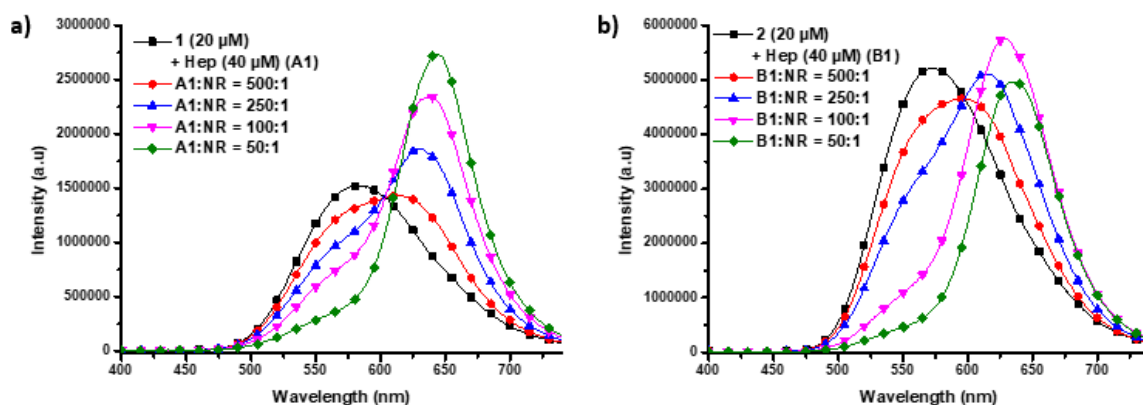


Fig. S11. Emission spectral changes of (a) **1** (20 μ M)-**Hep** (40 μ M) and (b) **2** (20 μ M)-**Hep** (40 μ M) in presence of **NR** at different D/A ratio in aqueous buffer.

Table S7. ET efficiency (%) and Antenna effect (AE) values in **1** (20 μ M)-**Hep** (40 μ M)-**NR** system at different donor/acceptor ratios.

Donor/acceptor ratio	ET efficiency	AE
500:1	13%	27
250:1	26%	40
100:1	39%	34
50:1	66%	23

Table S8. ET efficiency (%) and Antenna effect (AE) values in **2** (20 μ M)-**Hep** (40 μ M)-**NR** system at different donor/acceptor ratios.

Donor/acceptor ratio	ET efficiency	AE
500:1	16%	25
250:1	32%	31
100:1	69%	30
50:1	86%	19

Table S9. ET efficiency (%) and Antenna effect (AE) values in **1** (10 μ M)-**Hep** (20 μ M)-**NB** system at different donor/acceptor ratios.

Donor/acceptor ratio	ET efficiency	AE
500:1	18%	36
250:1	36%	45
100:1	61%	40
50:1	88%	20

Table S10. ET efficiency (%) and Antenna effect (AE) values in **2** (10 μ M)-**Hep** (20 μ M)-**NB** system at different donor/acceptor ratios.

Donor/acceptor ratio	ET efficiency	AE
500:1	17%	59
250:1	38%	69
100:1	77%	53
50:1	93%	27

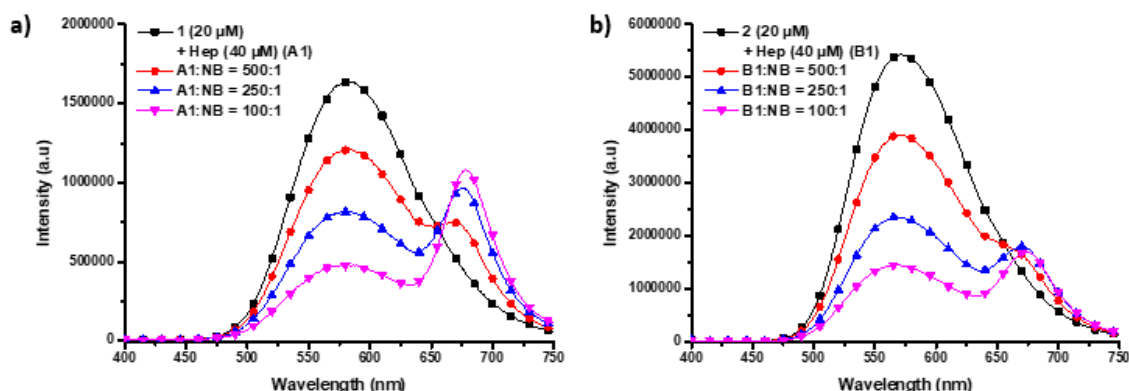


Fig. S12. Emission spectral changes of (a) **1** (20 μ M)-**Hep** (40 μ M) and (b) **2** (20 μ M)-**Hep** (40 μ M) in presence of **NB** at different D/A ratio in aqueous buffer.

Table S11. ET efficiency (%) and Antenna effect (AE) values in **1** (20 μ M)-**Hep** (40 μ M)-**NB** system at different donor/acceptor ratios.

Donor/acceptor ratio	ET efficiency	AE
500:1	26%	42
250:1	51%	42
100:1	71%	32

Table S12. ET efficiency (%) and Antenna effect (AE) values in **2** (20 μM)-Hep (40 μM)-NB system at different donor/acceptor ratios.

Donor/acceptor ratio	ET efficiency	AE
500:1	28%	58
250:1	57%	52
100:1	73%	41

Table S13. Lifetime data of **1** (10 μM)-Hep (20 μM) and **2** (10 μM)-Hep (20 μM) in presence of NR and NB in aqueous buffer ($\lambda_{\text{ex}} = 375 \text{ nm}$).

System	λ_{em}	Lifetime (τ) parameters	Average lifetime (τ_{avg})	χ^2
1 (10 μM)-Hep (20 μM)-NR (0.2 μM)	585 nm	$\tau_1 = 1.03 \text{ ns}$ (23%) $\tau_2 = 5.78 \text{ ns}$ (77%)	4.68 ns	1.27
2 (10 μM)-Hep (20 μM)-NR (0.2 μM)	572 nm	$\tau_1 = 0.52 \text{ ns}$ (28%) $\tau_2 = 1.93 \text{ ns}$ (72%)	1.54 ns	1.06
1 (10 μM)-Hep (20 μM)-NB (0.2 μM)	585 nm	$\tau_1 = 1.07 \text{ ns}$ (40%) $\tau_2 = 4.46 \text{ ns}$ (45%) $\tau_3 = 2.19 \text{ ns}$ (15%)	2.76 ns	1.14
2 (10 μM)-Hep (20 μM)-NB (0.2 μM)	572 nm	$\tau_1 = 3.24 \text{ ns}$ (40%) $\tau_2 = 1.29 \text{ ns}$ (60%)	2.07 ns	1.13

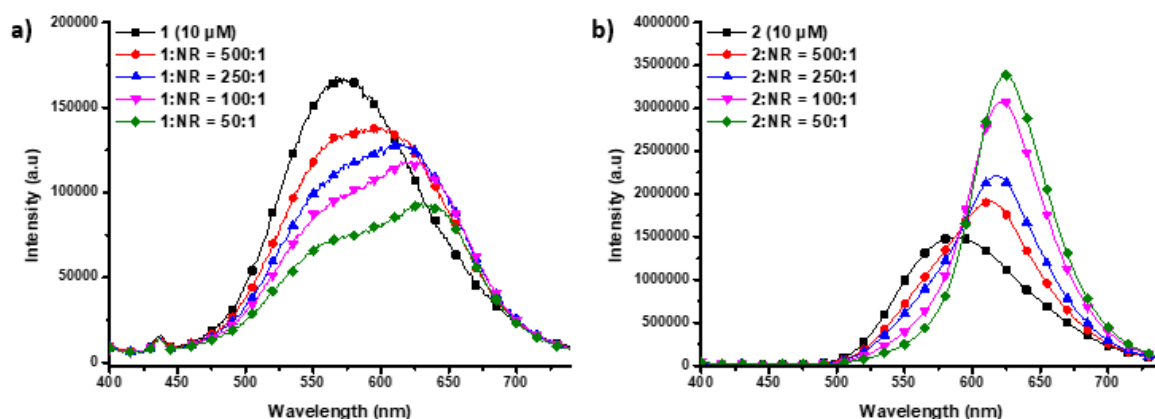


Fig. S13. Emission spectral changes of (a) **1** (10 μM) and (b) **2** (10 μM) in presence of NR at different D/A ratio in aqueous buffer.

Table S14. ET efficiency (%) and Antenna effect (AE) values in **1** (10 μM)-NR system at different donor/acceptor ratios.

Donor/acceptor ratio	ET efficiency	AE
500:1	19%	7
250:1	31%	5
100:1	41%	4.3
50:1	55%	1.5

Table S15. ET efficiency (%) and Antenna effect (AE) values in **2** (10 μ M)-**NR** system at different donor/acceptor ratios.

Donor/acceptor ratio	ET efficiency	AE
500:1	3%	30
250:1	9%	17
100:1	16%	20
50:1	31%	18

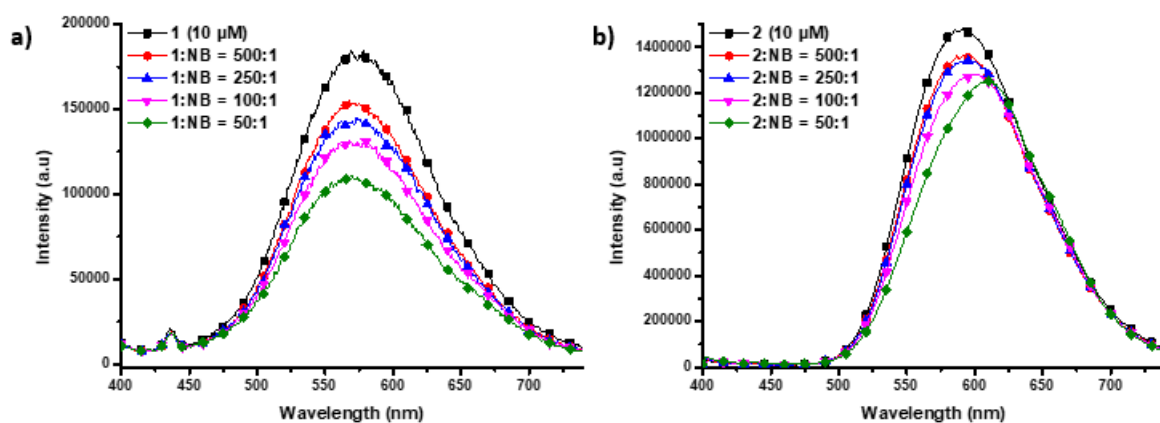


Fig. S14. Emission spectral changes of (a) **1** (10 μ M) and (b) **2** (10 μ M) in presence of **NB** at different D/A ratio in aqueous buffer.

Table S16. ET efficiency (%) and Antenna effect (AE) values in **1** (10 μ M)-**NB** system at different donor/acceptor ratios.

Donor/acceptor ratio	ET efficiency	AE
500:1	16%	0.3
250:1	22%	0.1
100:1	29%	0.2
50:1	40%	0.1

Table S17. ET efficiency (%) and Antenna effect (AE) values in **2** (10 μ M)-**NB** system at different donor/acceptor ratios.

Donor/acceptor ratio	ET efficiency	AE
500:1	8.2%	2.6
250:1	10%	2.5
100:1	15%	3.1
50:1	40%	4

Table S18. Steady-state fluorescence anisotropy (r) values of **NR** and **NB** in presence of **1** (10 μ M)-**Hep** (20 μ M) and **2** (10 μ M)-**Hep** (20 μ M) co-assemblies in buffer.

System	λ_{ex}	λ_{em}	r
1 (10 μ M)- Hep (20 μ M)- NR (200 nM)	586 nm	640 nm	0.172
2 (10 μ M)- Hep (20 μ M)- NR (200 nM)	586 nm	640 nm	0.161
1 (10 μ M)- Hep (20 μ M)- NB (200 nM)	635 nm	675 nm	0.117
2 (10 μ M)- Hep (20 μ M)- NB (200 nM)	635 nm	675 nm	0.151

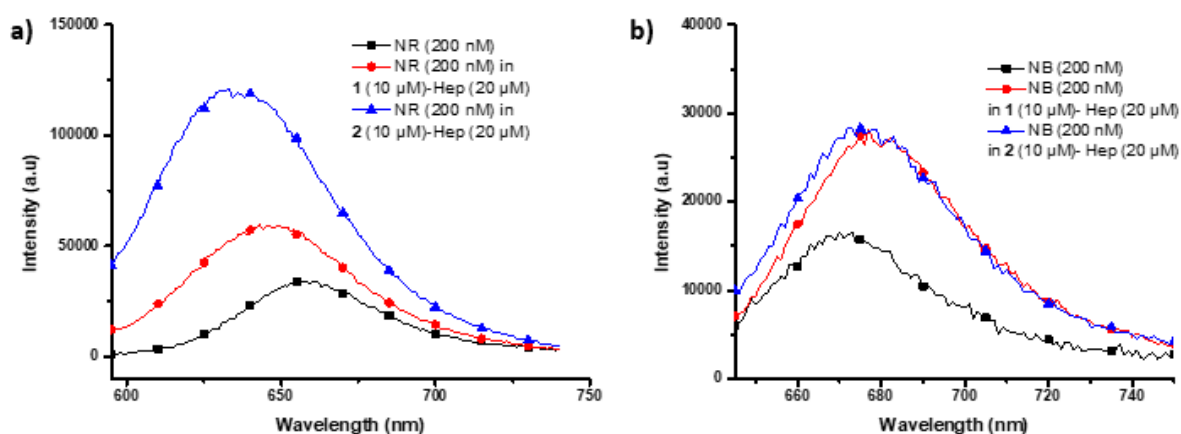


Fig. S15. Emission spectral changes of (a) **NR** (200 nM) and (b) **NB** (200 nM) in the absence and the presence of **1** (10 μ M)-**Hep** (20 μ M) and **2** (10 μ M)-**Hep** (20 μ M) co-assemblies in aqueous buffer.

Table S19. Steady-state fluorescence anisotropy (r) values of **NR** and **NB** in presence of **1** (10 μ M) and **2** (10 μ M) in buffer.

System	λ_{ex}	λ_{em}	r
1 (10 μ M)- NR (200 nM)	586 nm	640 nm	0.070
2 (10 μ M)- NR (200 nM)	586 nm	640 nm	0.183
1 (10 μ M)- NB (200 nM)	635 nm	675 nm	0.145
2 (10 μ M)- NB (200 nM)	635 nm	675 nm	0.147

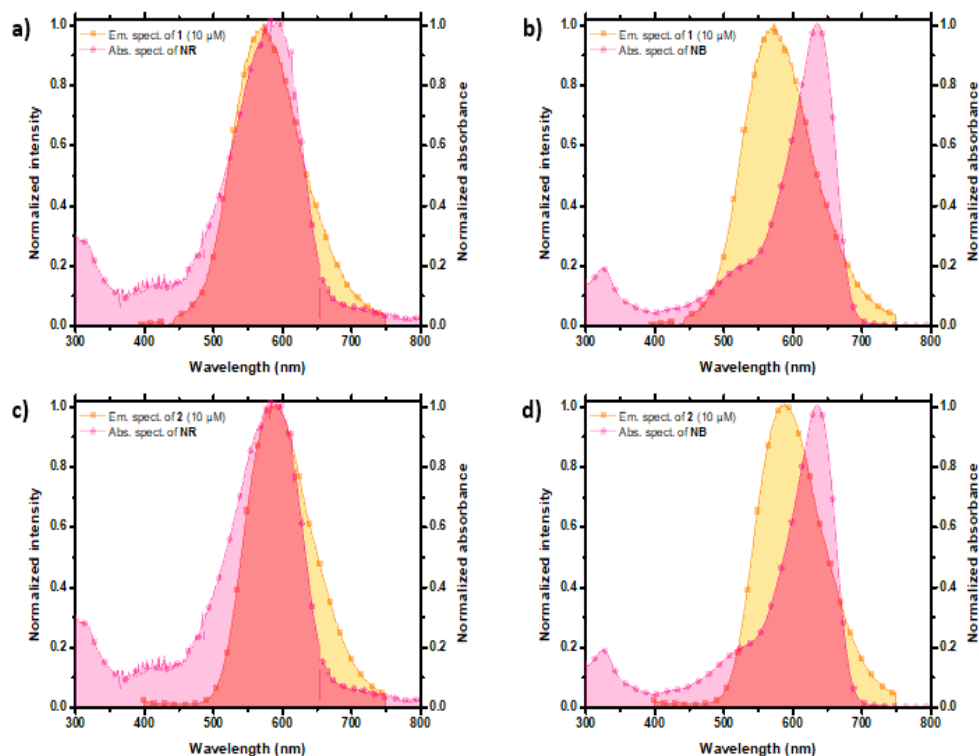


Fig. S16. Spectral overlap of emission of **1** (10 μ M) and absorption of (a) Nile Red (**NR**) and (b) Nile Blue (**NB**) in aqueous buffer. Spectral overlap of emission of **2** (10 μ M) and absorption of (c) Nile Red (**NR**) and (d) Nile Blue (**NB**) in aqueous buffer.

Spectral overlap between the co-assemblies and the acceptor dyes:

The overlap integral [$J(\epsilon)$] values of the emission spectra of **1** and **2** and the absorption spectra of the acceptor dyes were calculated by FluorTools software.

Table S20. Overlap integral [$J(\epsilon)$] of the emission spectra of **1** (10 μ M) and **2** (10 μ M) and the absorption spectra of the acceptor dyes

Self-assembly	Nile Red (NR)	Nile Blue (NB)
1 (10 μ M)	$9.42 \times 10^{-14} \text{ M}^{-1}\text{cm}^3$	$5.86 \times 10^{-13} \text{ M}^{-1}\text{cm}^3$
2 (10 μ M)	$1 \times 10^{-13} \text{ M}^{-1}\text{cm}^3$	$7.12 \times 10^{-13} \text{ M}^{-1}\text{cm}^3$

Calculation of the radiative rate constant (k_r) for **1** (10 μM):

Radiative rate constant (k_r) of donor [**1** (10 μM)] is calculated using following equation: $k_r = Q_D/\tau$

where, Q_D = Quantum efficiency of donor [**1** (10 μM)] = 0.0053

τ = Average lifetime of the donor [**1** (10 μM)] = 3.34 ns

The radiative rate constant (k_r) of **1** (10 μM) is determined to be $1.59 \times 10^6 \text{ s}^{-1}$.

Calculation of the radiative rate constant (k_r) for **2** (10 μM):

Radiative rate constant (k_r) of donor [**2** (10 μM)] is calculated using following equation: $k_r = Q_D/\tau$

where, Q_D = Quantum efficiency of donor [**2** (10 μM)] = 0.1432

τ = Average lifetime of the donor [**2** (10 μM)] = 2.54 ns

The radiative rate constant (k_r) of **2** (10 μM) is determined to be $5.64 \times 10^7 \text{ s}^{-1}$.

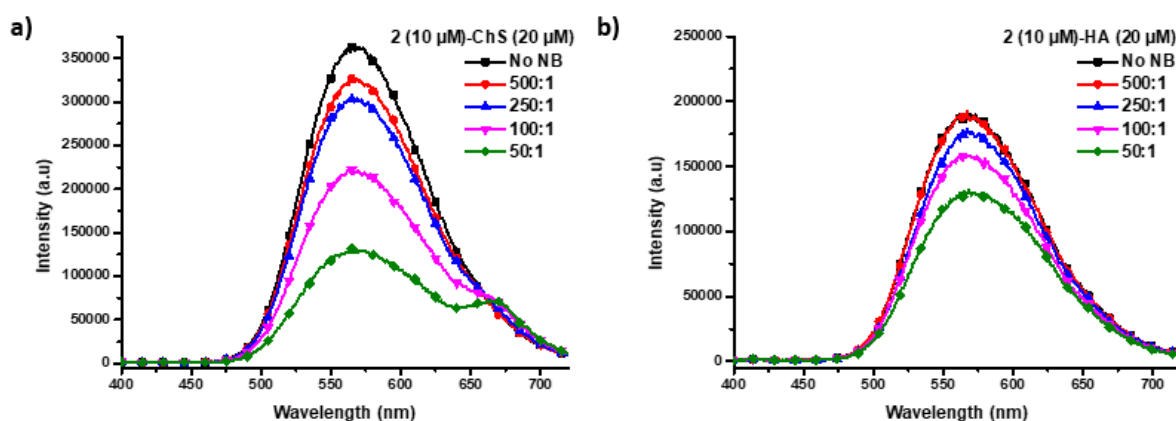


Fig. S17. Emission spectral changes of (a) **2** (10 μM)-ChS (20 μM) and (b) **2** (10 μM)-HA (20 μM) in presence of NB at different D/A ratio in aqueous buffer.

Table S21. ET efficiency (%) values in **2** (10 μM)-polyanion (20 μM) systems in the presence of NB in aqueous buffer at different donor/acceptor ratios.

Donor/acceptor ratio	Hep	ChS	HA
500:1	17%	16%	2%
250:1	38%	29%	8%
100:1	77%	69%	17%
50:1	93%	86%	30%

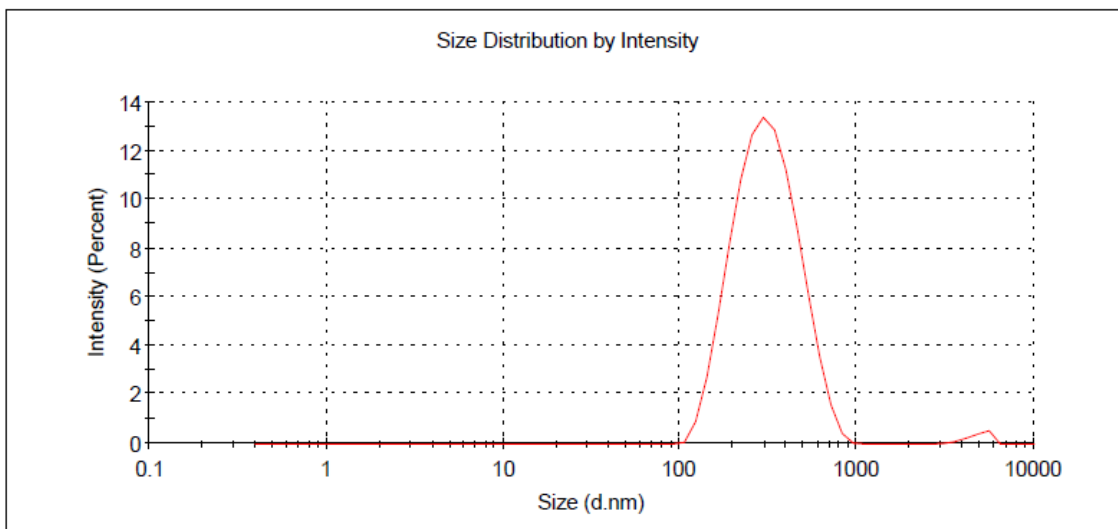
4. DLS Measurements:

A. Size measurements:

I. 1 (10 μ M) in buffer

Results

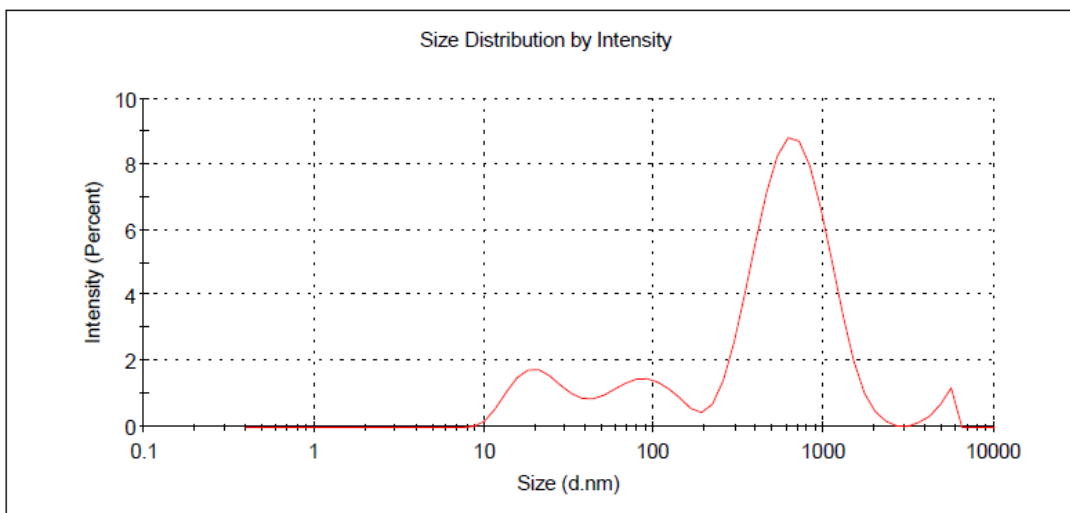
	Size (d.nm):	% Intensity:	St Dev (d.n...)
Z-Average (d.nm): 273.4	Peak 1: 327.9	98.6	133.4
Pdl: 0.260	Peak 2: 4852	1.4	699.6
Intercept: 0.928	Peak 3: 0.000	0.0	0.000
Result quality : Good			



II. 1 (10 μ M)-Hep (20 μ M) in buffer

Results

	Size (d.nm):	% Intensity:	St Dev (d.n...)
Z-Average (d.nm): 183.3	Peak 1: 717.7	73.7	352.4
Pdl: 1.000	Peak 2: 23.61	12.3	9.096
Intercept: 0.892	Peak 3: 92.99	11.6	37.92
Result quality : Refer to quality report			

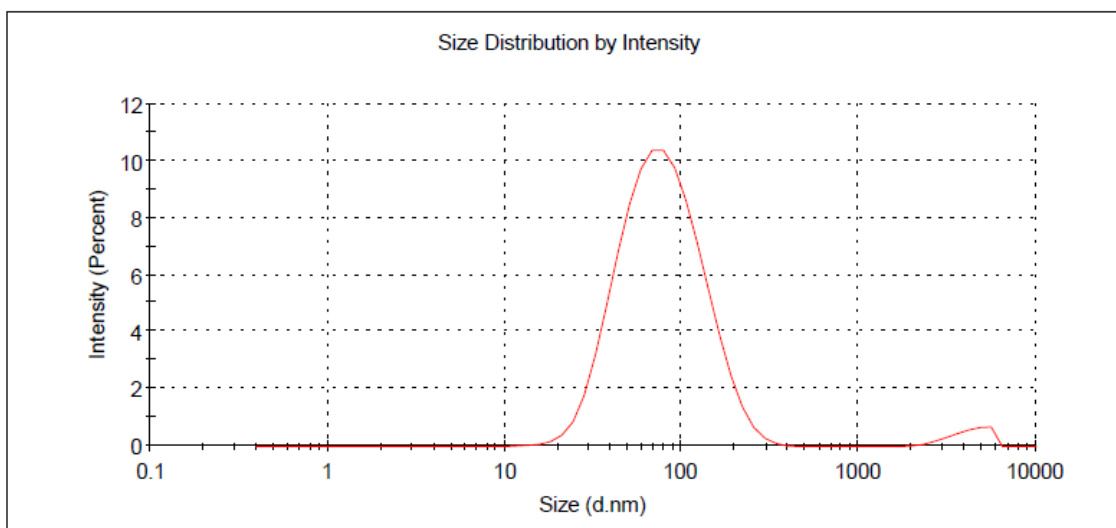


III. 2 (10 μ M) in buffer

Results

	Size (d.nm):	% Intensity:	St Dev (d.n...)
Z-Average (d.nm): 68.27	Peak 1: 86.16	97.0	46.93
Pdl: 0.260	Peak 2: 4274	3.0	977.9
Intercept: 0.947	Peak 3: 0.000	0.0	0.000

Result quality : **Good**

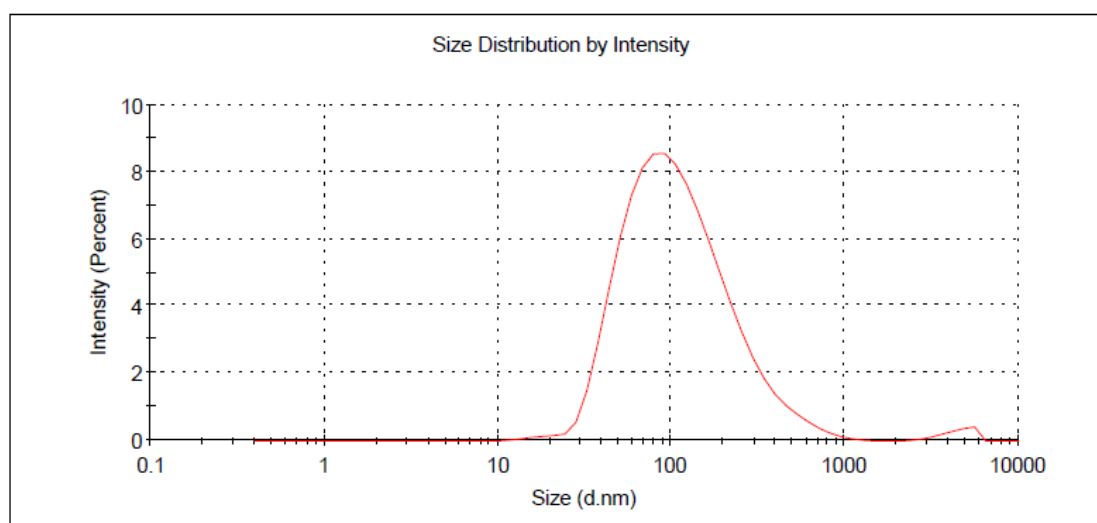


IV. 2 (10 μ M)-Hep (20 μ M) in buffer

Results

	Size (d.nm):	% Intensity:	St Dev (d.n...)
Z-Average (d.nm): 90.33	Peak 1: 135.8	98.6	118.1
Pdl: 0.289	Peak 2: 4521	1.4	876.7
Intercept: 0.948	Peak 3: 0.000	0.0	0.000

Result quality : **Good**

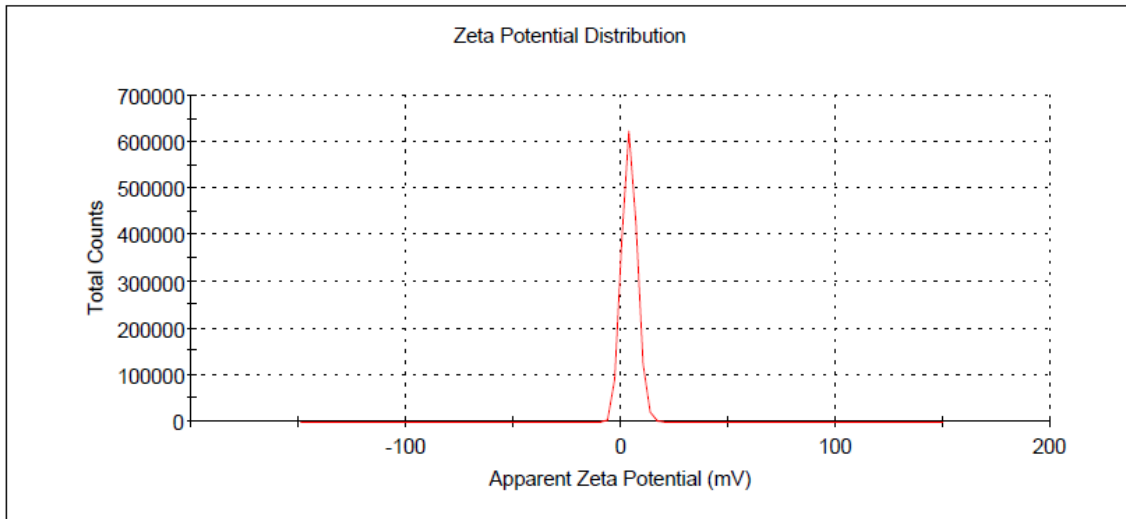


B. Zeta measurements:

I. 1 (10 μ M) in buffer

Results

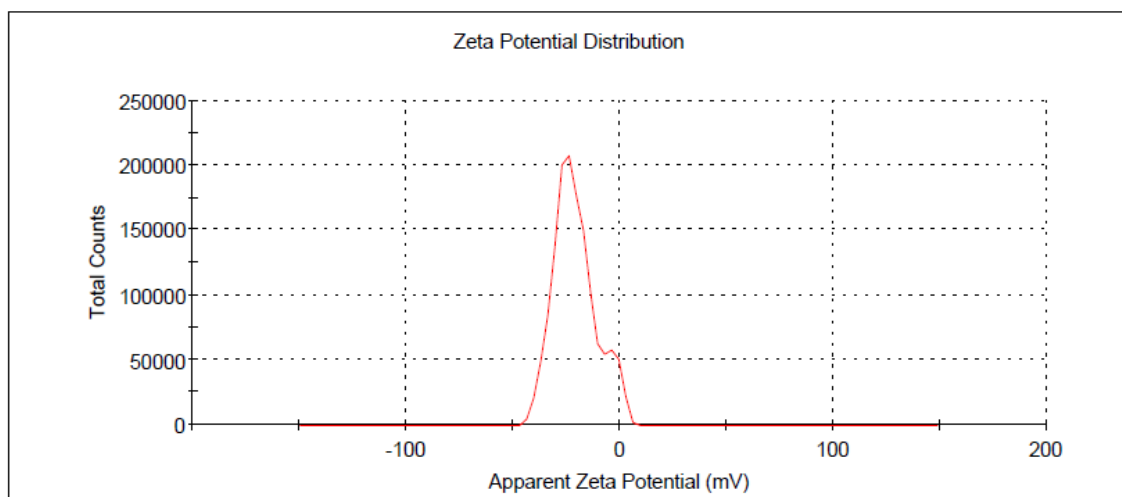
	Mean (mV)	Area (%)	St Dev (mV)
Zeta Potential (mV): 3.99	Peak 1: 3.98	100.0	3.58
Zeta Deviation (mV): 3.44	Peak 2: 0.00	0.0	0.00
Conductivity (mS/cm): 0.425	Peak 3: 0.00	0.0	0.00
Result quality: Good			



II. 1 (10 μ M)-Hep (20 μ M) in buffer

Results

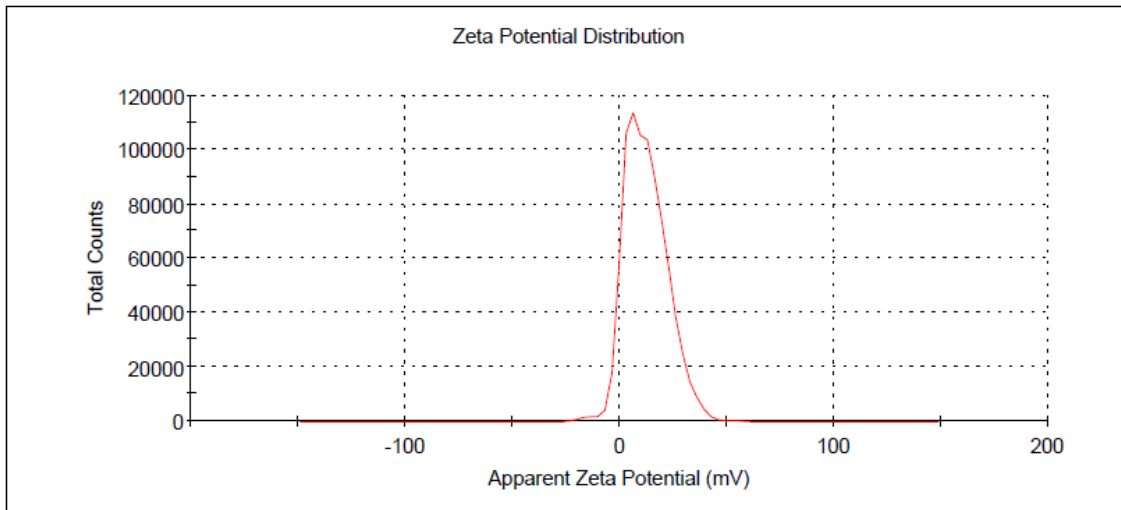
	Mean (mV)	Area (%)	St Dev (mV)
Zeta Potential (mV): -20.8	Peak 1: -23.0	94.3	7.86
Zeta Deviation (mV): 9.78	Peak 2: 0.724	5.7	1.83
Conductivity (mS/cm): 0.430	Peak 3: 0.00	0.0	0.00
Result quality: Good			



III. 2 (10 μ M) in buffer

Results

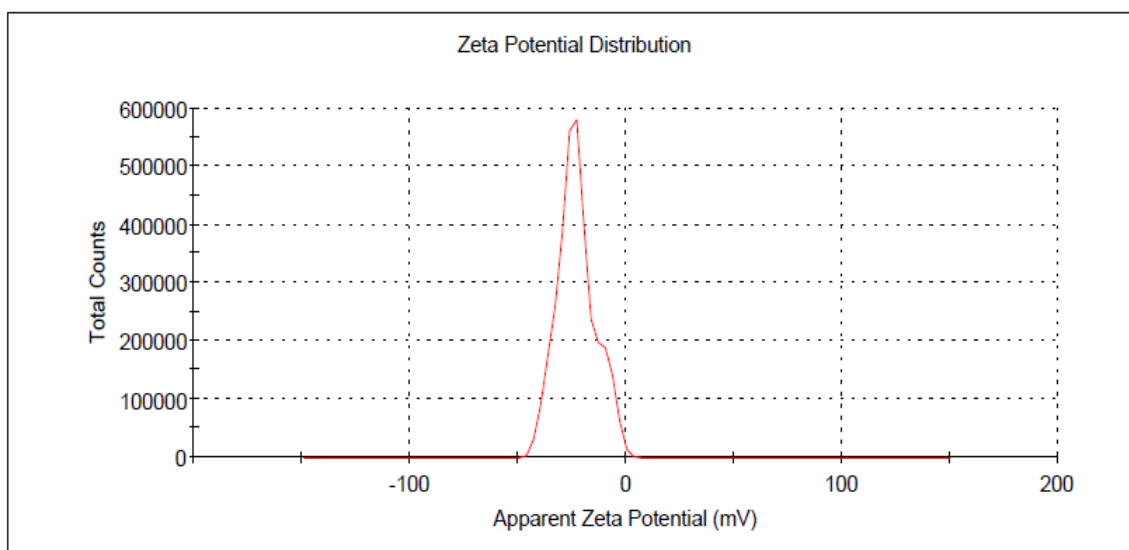
	Mean (mV)	Area (%)	St Dev (mV)
Zeta Potential (mV): 13.6	Peak 1: 12.3	100.0	9.72
Zeta Deviation (mV): 10.7	Peak 2: 56.5	0.0	1.31
Conductivity (mS/cm): 0.386	Peak 3: 0.00	0.0	0.00
Result quality : Good			



IV. 2 (10 μ M)-Hep (20 μ M) in buffer

Results

	Mean (mV)	Area (%)	St Dev (mV)
Zeta Potential (mV): -22.9	Peak 1: -22.9	100.0	8.85
Zeta Deviation (mV): 8.64	Peak 2: 0.00	0.0	0.00
Conductivity (mS/cm): 0.396	Peak 3: 0.00	0.0	0.00
Result quality : Good			



5. Time-correlated Single Photon Counting (TCSPC) Measurements:

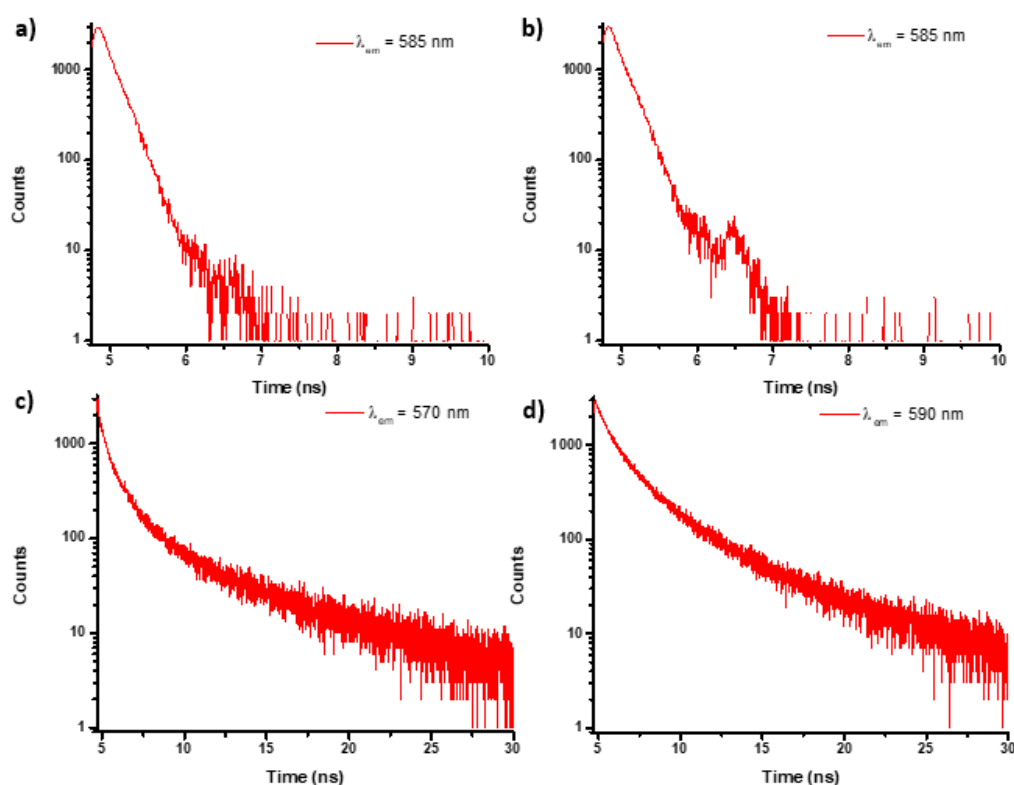


Fig. S18. Time-resolved emission decay profile of **1** (10 μM) in (a) DMSO and (c) buffer. Time-resolved emission decay profile of **2** (10 μM) in (b) DMSO and (d) buffer. ($\lambda_{\text{ex}} = 375 \text{ nm}$).

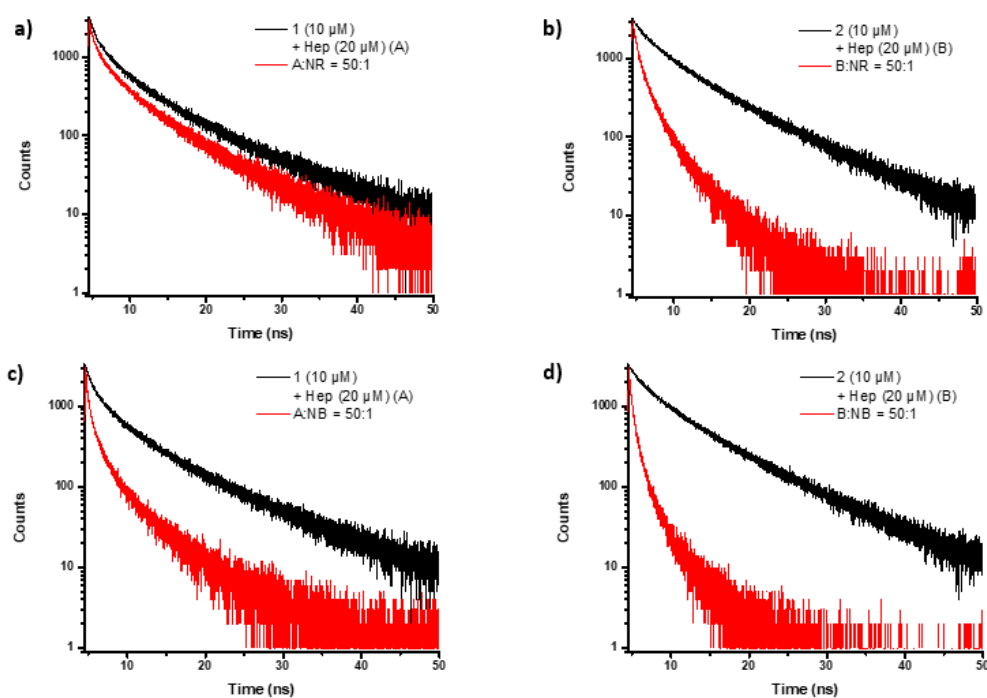
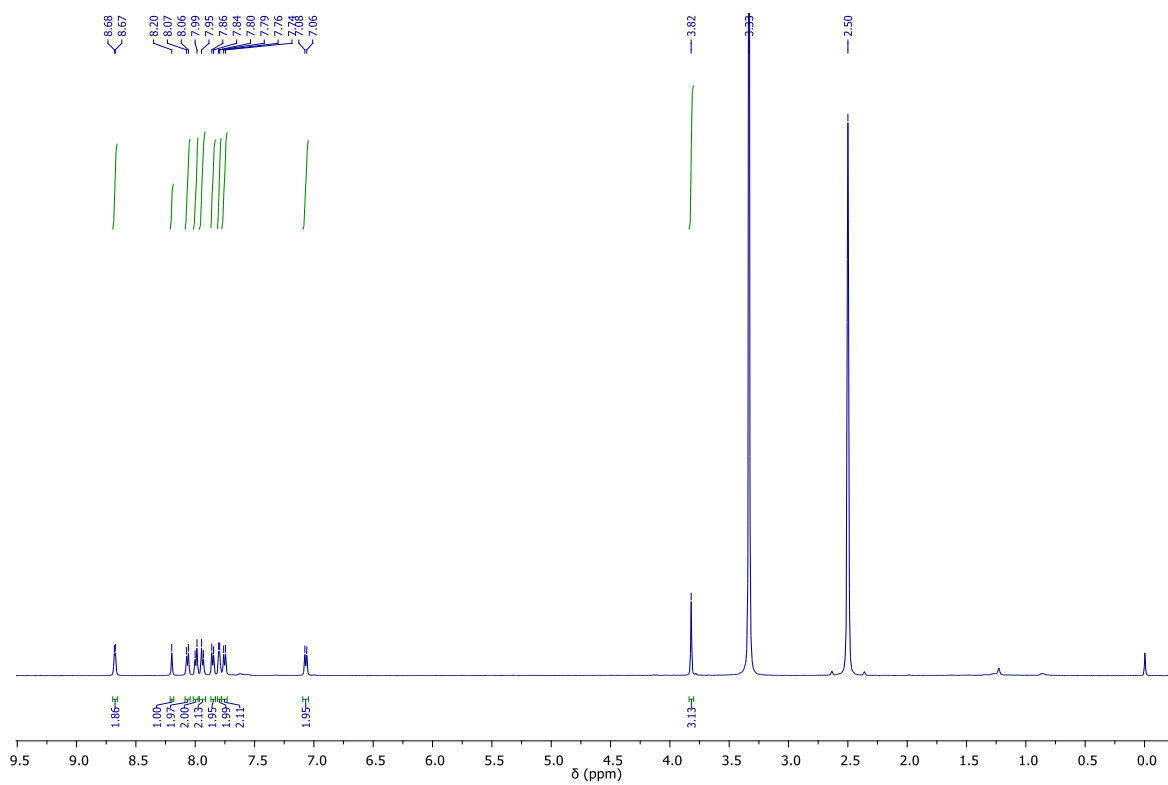
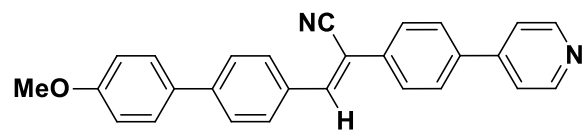


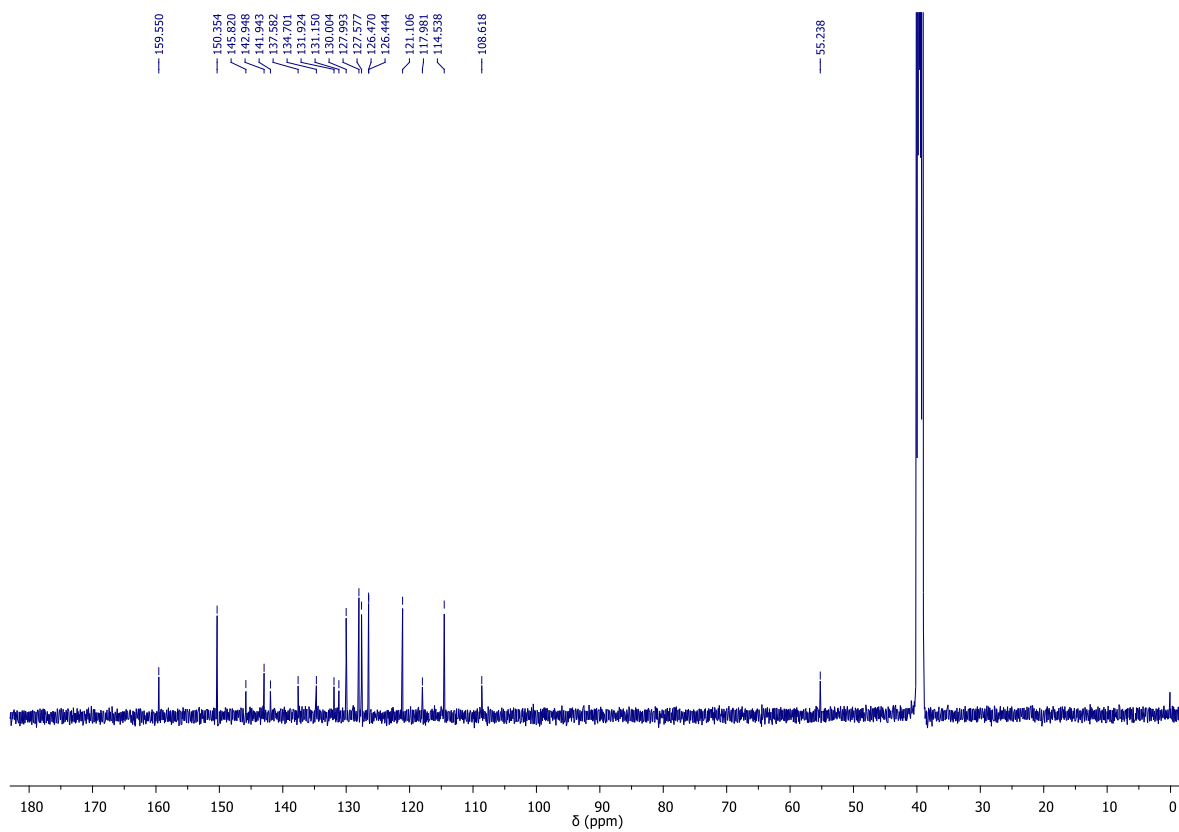
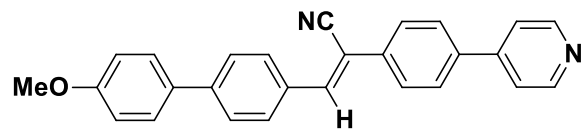
Fig. S19. Time-resolved emission decay profile of **1** (10 μM)-**Hep** (20 μM) in absence and presence of (a) **NR** (D/A = 50:1) and (c) **NB** (D/A = 50:1) in aqueous buffer. Time-resolved emission decay profile of **2** (10 μM)-**Hep** (20 μM) in presence of (b) **NR** (D/A = 50:1) and (d) **NB** (D/A = 50:1) in aqueous buffer.

6. NMR Spectra:

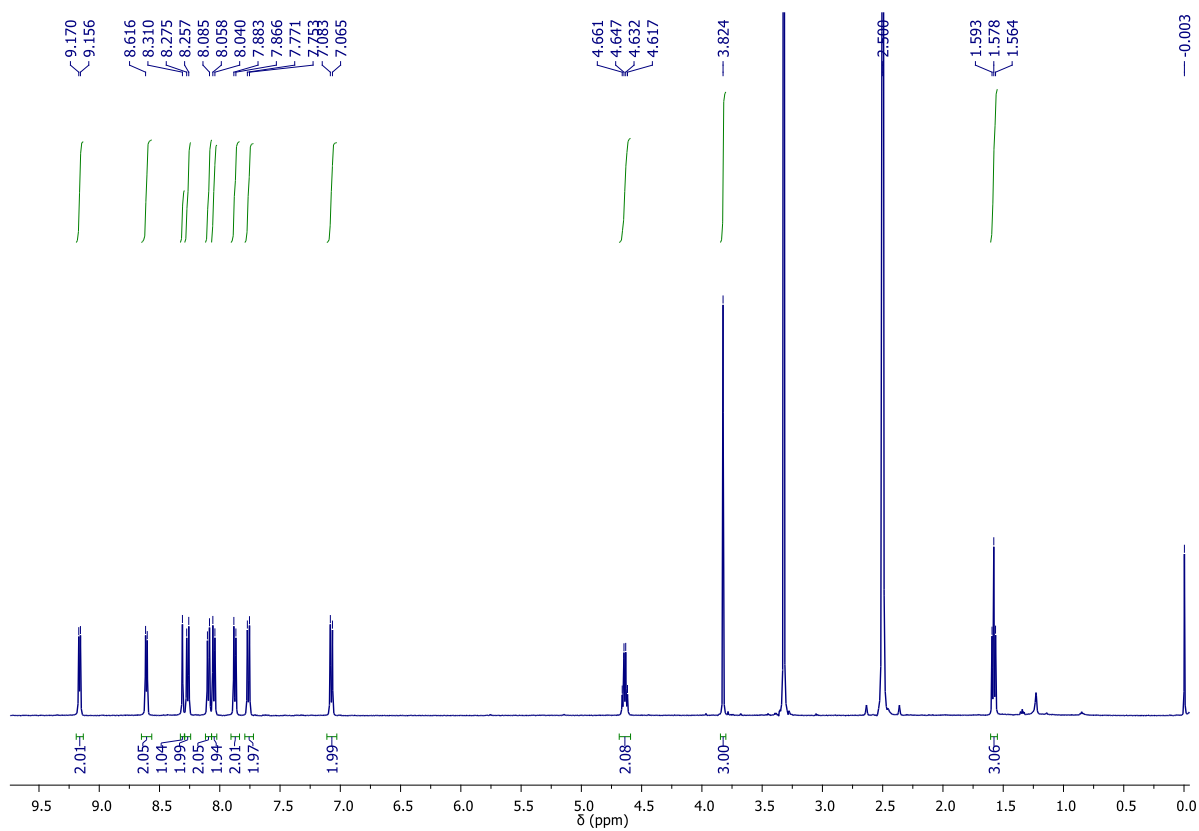
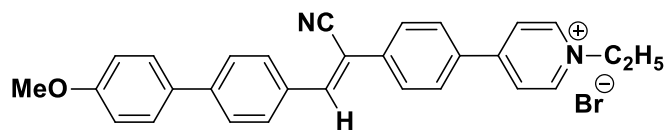
I. ^1H NMR of E (500 MHz, DMSO- D_6)



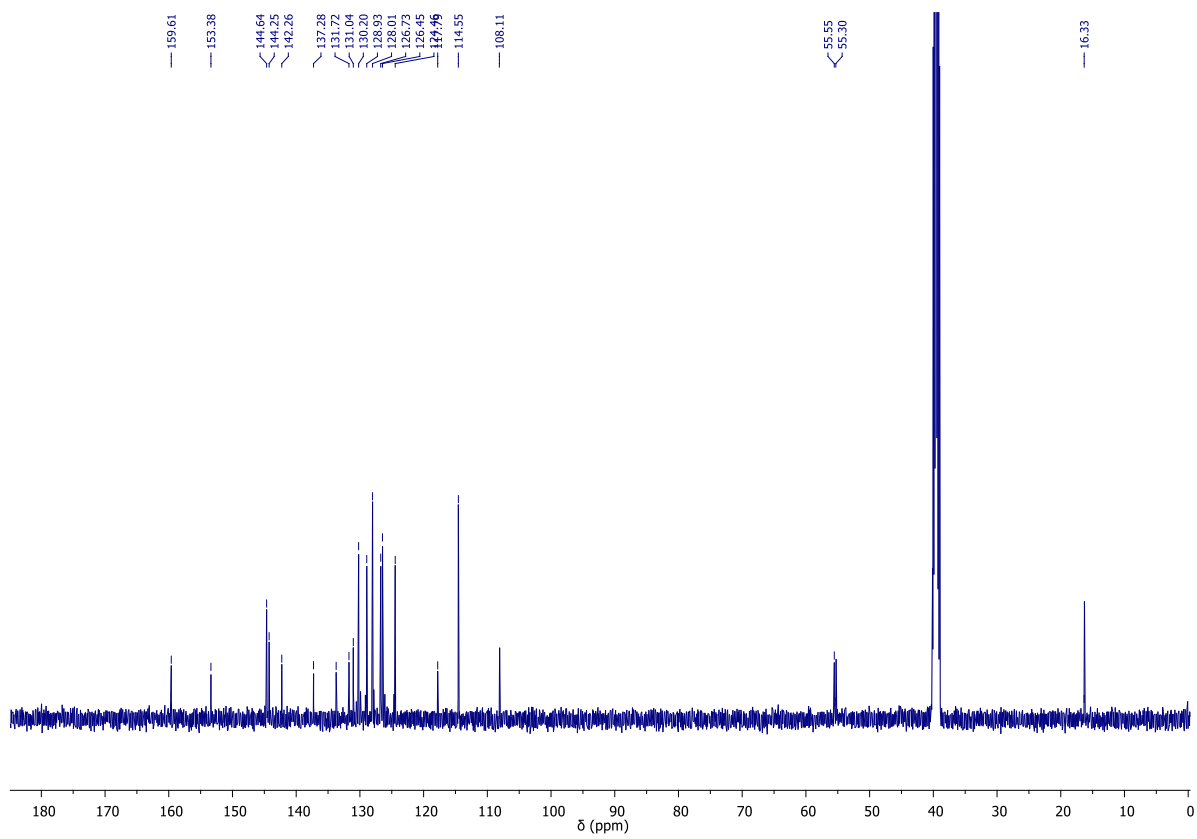
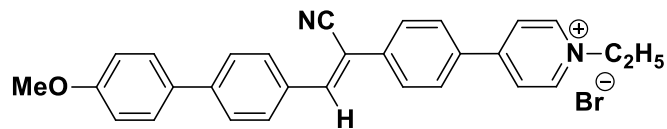
II. ^{13}C NMR of E (125 MHz, $\text{DMSO-}d_6$)



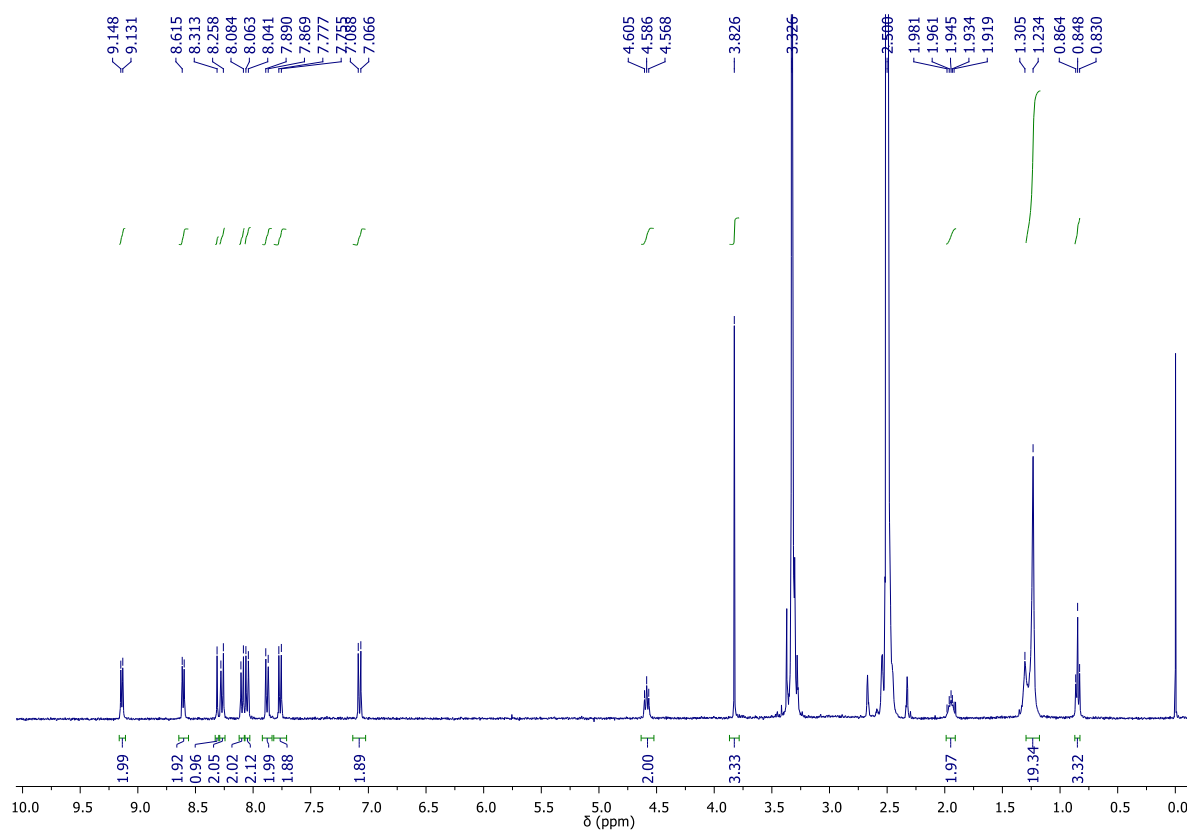
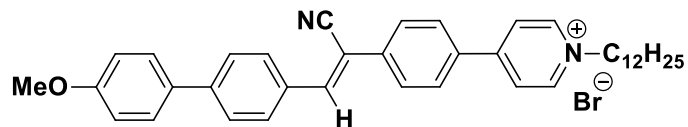
III. ^1H NMR of 1 (400 MHz, DMSO- D_6)



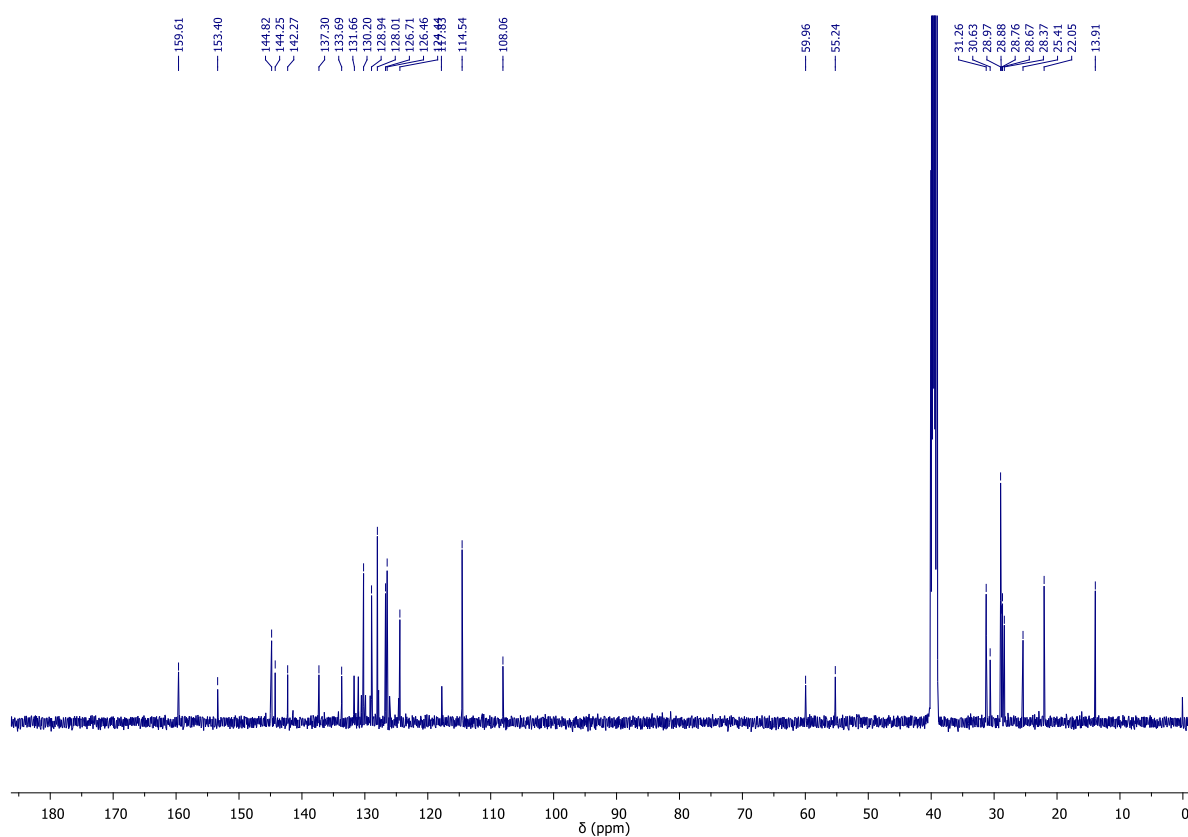
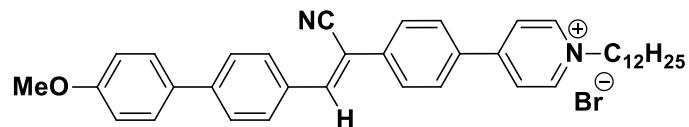
IV. ^{13}C NMR of 1 (125 MHz, $\text{DMSO-}D_6$)



V. ¹H NMR of 2 (400 MHz, DMSO-D₆)



VI. ^{13}C NMR of 2 (125 MHz, $\text{DMSO-}d_6$)



Reference

- (1) Y. You, H. Yang, J. W. Chung, J. H. Kim, Y. Jung and S. Y. Park, *Angew. Chem. Int. Ed.*, 2010, **49**, 3757.
- (2) G. L. Long and J. D. Winefordner, *Anal. Chem.*, 1983, **55**, 712A.